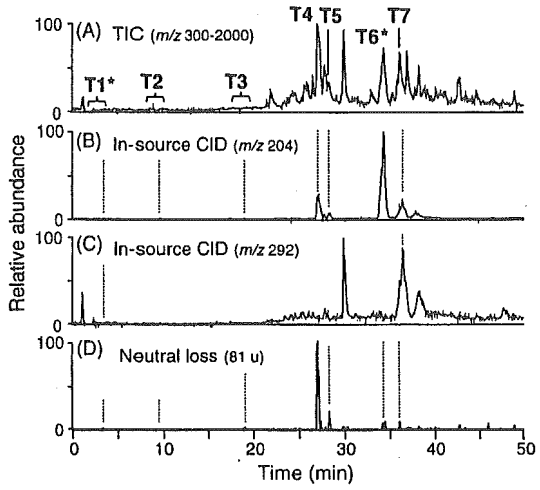

Fig. 2. Total ion chromatogram (TIC) of trypsin-digested protein at 20–25 kDa (*m/z* 300–2000) (A), mass chromatograms from TIC with ion-source CID of *m/z* 204 (B) and 292 (C), and neutral loss chromatogram of 81 u by data-dependent CID-MS/MS (D). Asterisks mean the peak of glycopeptides identified by the database search analysis.

the glycopeptide Val89-Lys99 contains two Asn residues, Asn93 and 98, only Asn98 was identified as a glycosylation site because of detection of b and y ions modified with GlcNAc at Asm98.

Next, to study the site-specific glycosylation at Asn74 and 98, product ion spectra of glycopeptides were sorted from the numbers of product ion spectra acquired around peak T6 and T1. We sorted out product ion spectra of glycopeptides using B series ions, such as $Hex_1HexNAc_1^+$ and $Hex_2HexNAc_1^+$ (*m/z* 366 and 528) originated from glycopeptides by CID-MS/MS, as marker ions [23]. We could sort out 14 product ion spectra originated from glycopeptide Val69-Lys78 around peak T6. The monosaccharide compositions of *N*-glycans at Val69-Lys78 were calculated as $dHex_{0-3}Hex_{2-7}HexNAc_{2-5}$ on the basis of the *m/z* values of their molecular ions and the theoretical mass of the peptide. Likewise, seven product ion spectra originated from glycopeptide Val89-Lys99 were sorted from those around peak T1, and their monosaccharide compositions were estimated as $dHex_{0-2}Hex_{3,5,6}HexNAc_{2-5}NeuAc_{0,1}$ (Table 1). Glycosylation at Asn74 and 98 were elucidated by a detailed examination of these product ion spectra as follows.

3.2.1. Analysis of the glycosylation at Asn74 of peptide Val69-Lys78

Fig. 3(A) shows a product ion spectrum of the glycopeptide Val69-Lys78 at 34.52 min. Its precursor ion is the doubly charged ion at *m/z* 1512.2. Many product ions generated by cleavages of glycosidic linkages can be observed in this product ion spectrum. The most intense ion at *m/z* 1311 is assigned to a peptide bearing the reducing end of GlcNAc, which was caused by glycosidic linkage cleavage of *N*-linked oligosaccharide. Fig. 3(B) is the product ion spectrum of the peptide + GlcNAc ion at *m/z* 1311. The b and y ions generated by cleavages of the peptide backbone prove that this glycopeptide is the peptide Val69-Lys78 glycosylated at Asn74.

The molecular weight of the carbohydrate moiety can be calculated as 1933.8 Da by subtracting the theoretical mass of the peptide (1106.6 Da) from the calculated glycopeptide mass (3022.4 Da). Consequently, the monosaccharide composition can be estimated as $dHex_2Hex_5HexNAc_4$. In the product ion spectrum (Fig. 3(A)), B ions corresponding to $dHex_1Hex_1HexNAc_1$ ($B_{2\alpha}$) and $dHex_1Hex_2HexNAc_1$ ($B_{3\alpha}$) were detected at *m/z* 512 and 674, respectively. These results indicate that one of two dHex, which are likely to be Fuc, attaches to Gal-GlcNAc at the non-reducing end in a similar manner as the Lewis a/x antigen (Gal-(Fuc-)GlcNAc-), or the blood group H-determinant (Fuc-Gal-GlcNAc-). The product ion at *m/z* 350 produced from the triply charged precursor ion at *m/z* 1008.7 corresponded to $dHex_1HexNAc_1$ (data not shown), suggesting that Fuc attaches to GlcNAc like the Lewis a/x antigen (Gal-(Fuc-)GlcNAc-). The attachment site of the other Fuc can be deduced at inner trimannosyl core GlcNAc from the observation of Y ions at *m/z* 1457, 1660, and 1822, which correspond to Val69-Lys78 plus $dHex_1HexNAc_1$ ($Y_{1\alpha}$), $dHex_1HexNAc_2$ ($Y_{2\alpha}$), and $dHex_1Hex_1HexNAc_2$ ($Y_{3\alpha/3\beta/3\gamma}$), respectively. In addition, the product ion at *m/z* 1411 resulting from the precursor ion at *m/z* 1512.2 by loss of 101.6 u (HexNAc), suggests a linkage of non-substituted HexNAc at the non-reducing terminal end. Together with detection of the product ion at *m/z* 940 ($Y_{3\alpha/1\beta/3\beta}^+$, [GlcNAc-Man-GlcNAc-GlcNAc-peptide+H]$^{2+}$), it can be deduced that this HexNAc is a bisecting GlcNAc attached to the core mannose residue via a β1–4 linkage. From these product ions, we could deduce two oligosaccharide structures. One is the structure indicated in Fig. 3(A), inset, and the other is one containing a Gal-Gal-(Fuc-)GlcNAc-Man-branch instead of a Gal-(Fuc-)GlcNAc-Man-branch. Detection of Gal-(Fuc-)GlcNAc-Man$^+$ at *m/z* 674 but not Gal-Gal-(Fuc-)GlcNAc-Man$^+$ at *m/z* 836 suggests that this oligosaccharide structure can be assigned to the structure indicated in Fig. 3(A), inset.

The carbohydrate structures of the other glycopeptide Val69-Lys78 detected around peak T6 can be characterized as the high-mannose-type oligosaccharide (M5), complex-type oligosaccharides containing some partial structures such as inner core Fuc, bisecting GlcNAc, the Lewis a/x antigen, and blood group H-determinant, and hybrid-type oligosaccharides (Table 1).

3.2.2. Analysis of the glycosylation at Asn98 of peptide Val89-Lys99

Fig. 4 shows one of the product ion spectra of the glycopeptide Val89-Lys99 at 3.47 min. Its precursor ion is the doubly charged ion at *m/z* 1525.8. The monosaccharide composition, $dHex_1Hex_6HexNAc_4$, can be estimated based on the calculated mass of the carbohydrate moiety (1950.0 Da) obtained by subtracting the mass of the theo-

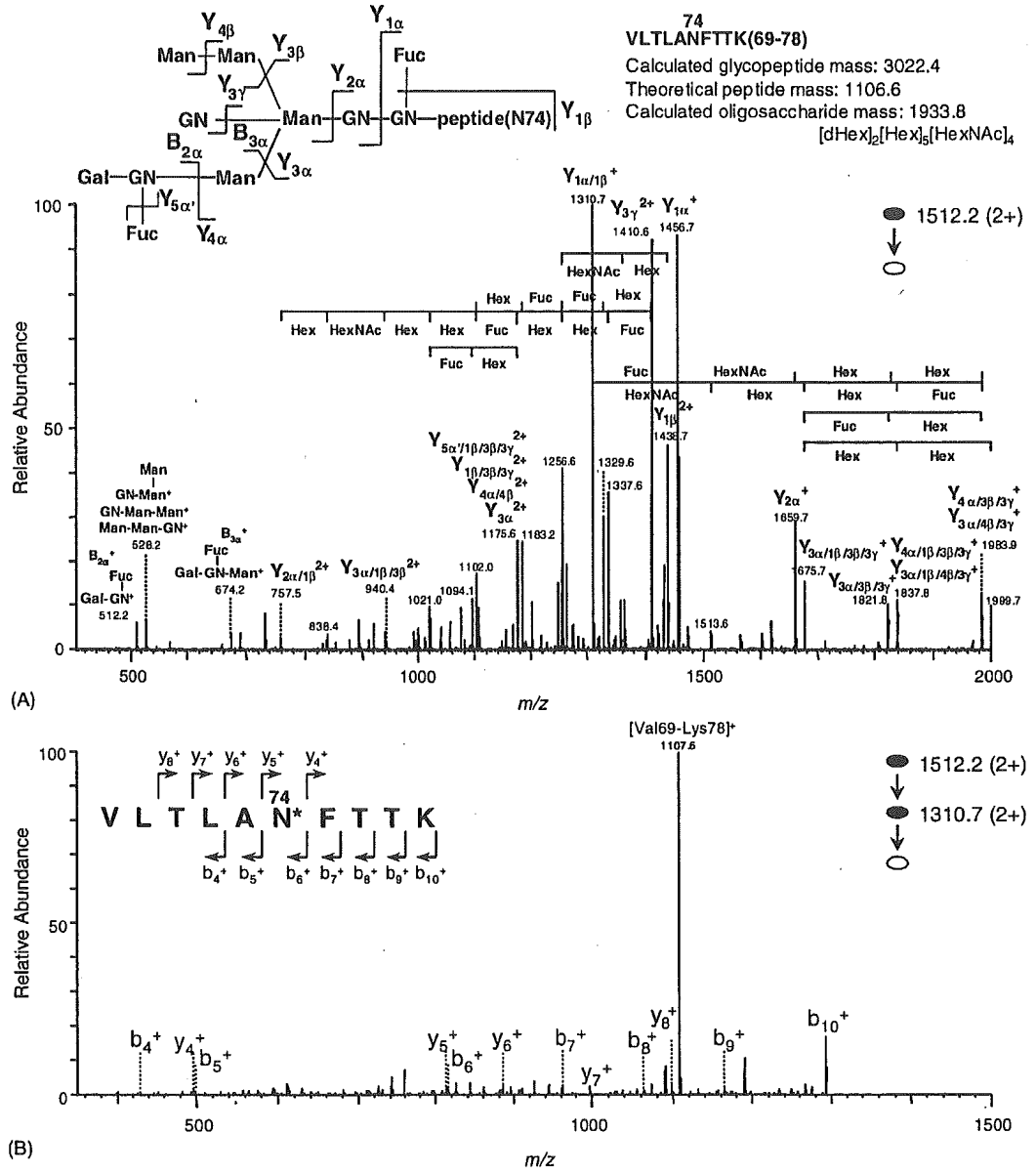

Fig. 3. (A) Product ion spectrum (MS^2) of the doubly charged glycopeptide precursor ion at *m/z* 1512.2 in peak T6. The glycopeptide Val69-Lys78 is glycosylated with oligosaccharide, $dHex_2Hex_5HexNAc_4$ at Asn74, and the inset is the deduced oligosaccharide structure. (B) MS^3 product ion spectrum derived from the doubly charged glycopeptide precursor ion at *m/z* 1512.2, followed by further fragmentation of the product ion at *m/z* 1310.7.

retical typtic peptide mass (1117.5 Da) from the calculated glycopeptide mass (3049.5 Da). Y ions corresponding to Val89-Lys99 plus $dHex_1HexNAc_1$ ($Y_{1\alpha}$), $dHex_1HexNAc_2$ ($Y_{2\alpha}$), and $dHex_1Hex_1HexNAc_2$ ($Y_{3\alpha/3\beta/3\gamma}$) detected at *m/z* 1468, 1671, and 1833, respectively, reveals that one Fuc residue is linked to the inner trimannosyl core GlcNAc. Additionally, the product ion at *m/z* 1424 suggests a linkage of non-substituted HexNAc at the non-reducing terminal end. Together with the product ions at *m/z* 945 and 1890, it can be deduced that this HexNAc is a bisecting GlcNAc that attaches to a core mannose residue via a β1–4 linkage. On the basis of the product ions at *m/z* 487, 528 and 1380, corresponding to Hex_3 ($B_{2\beta}$), $Hex_2HexNAc_1$ ($B_{3\alpha}$), and $Hex_6HexNAc_2$ ($B_{4\alpha}$), the oligosaccharide structure was characterized as a hybrid-type oligosaccharide (Fig. 4, inset).

The carbohydrate structures of the other glycopeptide Val89-Lys98 detected around peak T1 are characterized as high-mannose-type oligosaccharide (M5), complex-type, and hybrid-type oligosaccharides, which include bisecting GlcNAc and Lewis a/x structures (Table 1).

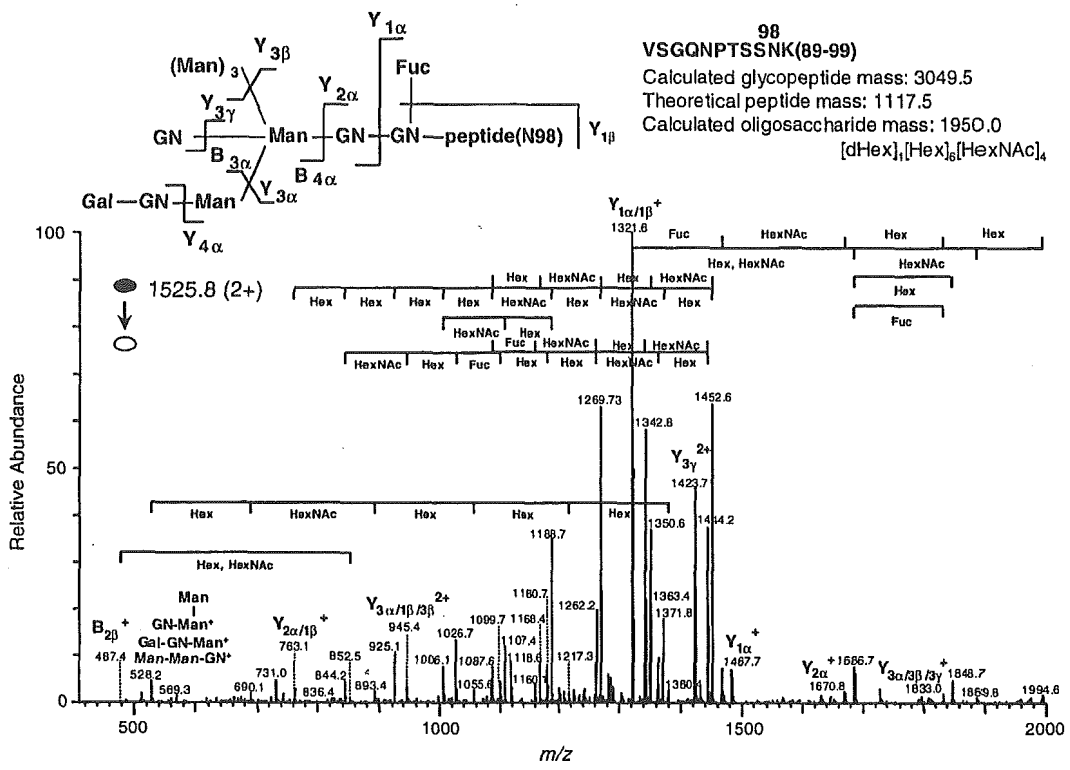

Fig. 4. Product ion spectrum of the doubly charged glycopeptide precursor ion at *m/z* 1525.8 in peak T1. The glycopeptide Val89-Lys99 is glycosylated with the oligosaccharide, $dHex_1Hex_6HexNAc_4$ at Asn98, and the inset is the deduced oligosaccharide structure.

3.3. Detection of glycopeptides by in-source CID and CID-MS/MS

Glycopeptides containing Asn23 could not be identified by the database search analysis. Therefore, we first localized all glycopeptides in the peptide/glycopeptide map using oxonium marker ions generated by in-source CID. Fig. 2(B and C) shows mass chromatograms of oxonium marker ions, $HexNAc^+$ (*m/z* 204) and $NeuAc^+$ (*m/z* 292), respectively. The mass chromatogram of *m/z* 204 indicates that the glycopeptides were localized around 3.7, 9.7, 19.1, 27.2, 28.4 34.3, 36.3, and 37.8 min. The mass chromatogram of *m/z* 292 suggests that the glycopeptides bearing NeuAc were localized around 3.7, 30.0, 36.4, and 38.2 min. In addition to the localization of glycopeptides by in-source CID, we monitored neutral loss caused by data-dependent CID-MS/MS. The neutral loss chromatogram of 81 u indicates the localization of doubly charged glycopeptides ions with Hex at the non-reducing ends. The elution positions of the localized glycopeptides by neutral loss are almost identical to those by in-source CID. Second, for confirmation of the elution position of glycopeptides and characterization of the carbohydrate moiety, we sorted the product ion spectra of glycopeptides from enormous numbers of data-dependently acquired product ion spectra around localized glycopeptides by using oligosaccharide oxonium ions as marker ions. Consequently, the locations of glycopeptides were confirmed in peak T1-6 (Fig. 2(A)). The peaks T1 and 6 correspond to the location of glycopeptides identified by the database search as Val89-Lys99 and Val69-Lys78, respectively. Four glycopeptide peaks were newly sorted by in-source CID and data-dependent CID-MS/MS. Structural assignment of the glycopeptides in these peaks was carried out using their MS^n spectra as follows.

3.3.1. Analysis of the glycosylation at Asn23 of peptide His21-Phe33

Fig. 5(A) shows one of the product ion spectra of the glycopeptide His21-Phe33 in peak T4. Its precursor ion is the triply charged ion at *m/z* 937.3. The intense product ion at *m/z* 899 is assigned to a doubly charged ion of peptide plus GlcNAc on the basis of Y series ions. The region of His21-Phe33 containing Asn23 in Thy-1 was suggested as the peptide moiety of this glycopeptide, 1593.3 Da, by the FindPept tool available on the internet (ExPASY Proteomics tools, Swiss Institute of Bioinformatics, http://us.expasy.org/tools/findpept.html). We examined the data-dependently acquired product ion spectrum of the precursor ion at *m/z* 899 and found that the *m/z* values of b and y ions in the product ion spectrum were identical to those of predictable product ions originating from the peptide His21-Phe33 modified with HexNAc at Asn23 (Fig. 5(B)). From the calculated oligosaccharide mass (1235.1 Da) obtained by subtracting the theoretical typtic

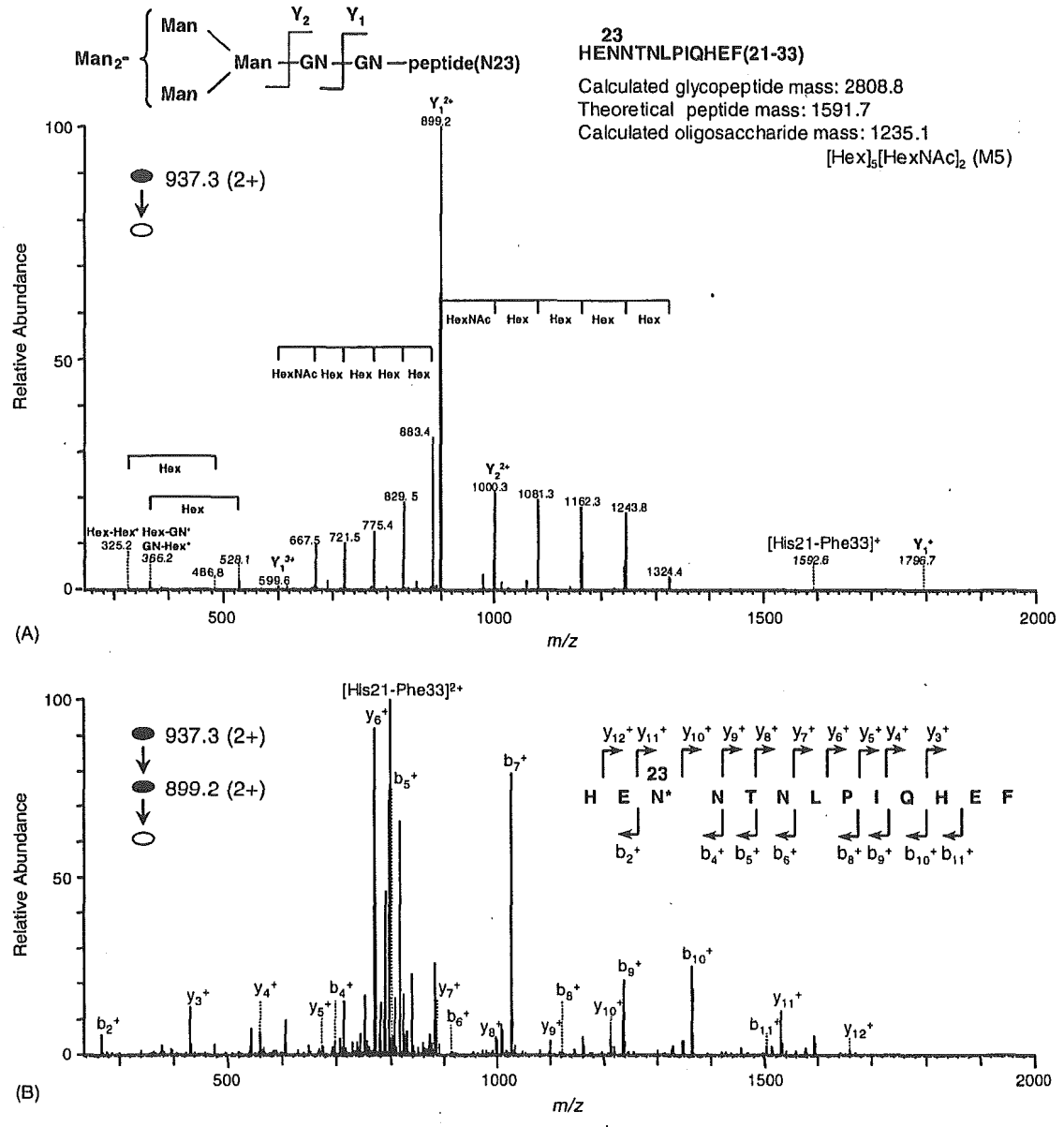

Fig. 5. (A) Product ion spectrum (MS^2) of the doubly charged glycopeptide precursor ion at *m/z* 937.3 in peak T4. The glycopeptide His21-Phe33 is glycosylated with oligosaccharide, $Hex_5HexNAc_2$ at Asn23, and the inset is the deduced oligosaccharide structure. (B) MS^3 product ion spectrum derived from a doubly charged glycopeptide precursor ion at *m/z* 937.3, followed by further fragmentation of the product ion at *m/z* 899.2.

peptide mass (1591.7 Da) from the calculated glycopeptide mass (2808.8 Da) together with product ions at *m/z* 366 and 528, it is indicated that this peptide carries $Hex_5HexNAc_2$, i.e. high-mannose-type oligosaccharide, M5. All product ion spectra in peak T4 revealed that peptides His21-Phe33 contain only high-mannose-type oligosaccharide (M5).

3.3.2. *Analysis of glycopeptides in peaks T2, 3, 5, and 7*

Similarly, product ion spectra of glycopeptides around peaks T2, 3, 5, and 7 were sorted by using oligosaccharide oxonium marker ions generated by MS/MS. In product ion spectra sorted out from around peak T2, the intense ion at *m/z* 884 was detected and assigned to a singly charged ion of a peptide plus GlcNAc. The peptide was suggested to be Ala73-Lys78 containing Asn74 by the FindPept tool. The monosaccharide composition can be estimated from the calculated mass of oligosaccharide moiety obtained by subtracting the theoretical mass of Ala73-Lys78 (680.35 Da) from calculated glycopeptide mass. Oligosaccharide structure of the glycopeptides is characterized based on their product

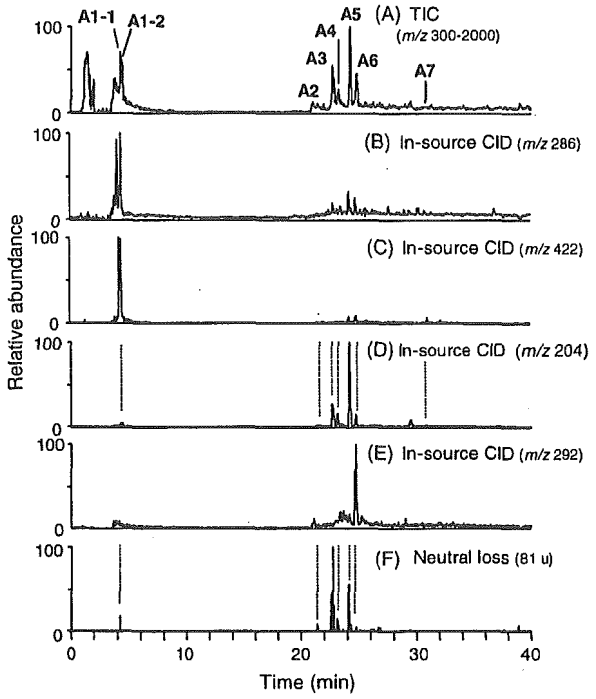

Fig. 6. Total ion chromatogram (TIC) of Asp-N digested protein at 20–25 kDa (*m/z* 300–2000) (A), mass chromatograms from TIC with in-source CID of *m/z* 286 (B), 422 (C), 204 (D), and 292 (E), and neutral loss chromatogram of 81 u by data-dependent CID-MS/MS (F).

ion spectra. Glycopeptides in peak T2 were characterized as Ala73-Lys78 glycosylated at Asn74 with *N*-glycans consisting of $dHex_{0-2}Hex_{3-6}HexNAc_{2-5}$. These *N*-glycans can be identified as high-mannose-type oligosaccharide (M5), and complex-type and hybrid-type oligosaccharides containing Fuc attached to inner trimannosyl core GlcNAc. Their structural assignments are summarized in Table 1. Glycopeptides in peak T3 can be identified as a mixture of peptide His21-His31 and His21-Glu32 glycosylated at Asn23, and Ser96-Asp106 glycosylated at Asn98. Asn23 was attached by high-mannose-type oligosaccharides, M5, 6, and 7, and Asn98 was occupied by *N*-glycan consisting of $dHex_1Hex_4HexNAc_4$ with a Lewis a/x structure as a partial structure. Glycopeptides in peak T5 were characterized as peptide His21-Phe33 glycosylated at Asn23 with high-mannose-type oligosaccharide, M6. Glycopeptides in peak T7 were assigned to be Val69-Lys78 glycosylated at Asn74 with *N*-glycans composed of $dHex_{1-2}Hex_{4-6}HexNAc_{3-6}NeuAc$.

3.4. Analysis of the GPI moiety of rat Thy-1

Since trypsin digestion provided Cys-GPI, which could not be retained on the C_{18} column, Asp-N digestion was also performed to obtain more hydrophobic peptides attached by GPI (GPI-peptides). Fig. 6(A) shows the peptide/glycopeptide map obtained by LC/ITMS of Asp-N digested Thy-1. We localize the GPI-peptides using marker ions, EtN-PO_4-Man$^+$ at *m/z* 286 and GlcN-inositol-PO_4^+ at *m/z* 422, originating from the core structure of the GPI moiety by in-source CID (EtN, ethanolamine; GlcN, glucosamine). Mass chromatograms of *m/z* 286 and 422 suggest the locations of the GPI-peptides to be around 4.2 (peak A1-1) and 4.4 min (peak A1-2) (Fig. 6(B and C)). Using product ions originated from GPI moiety, such as GlcN-inositol-PO_4^+ and PO_4-Man-GlcN$^+$ (*m/z* 422 and 404), as marker ions, four product ion spectra of GPI-peptides were sorted out from all product ion spectra around peaks A1-1 and 1-2. Their precursor ions were doubly charged ions at *m/z* 1132 and 1213 (peak A1-1), 1051 and 1151 (peak A1-2). Based on these product ion spectra, we characterized GPI-peptides as the peptide Asp106-Cys111 with a GPI core structure plus Hex_{0-2}, $HexNAc_{1-2}$ and PO_4-EtN.

Fig. 7(A) shows the product ion spectrum of the doubly charged GPI-peptide ion at *m/z* 1051 in peak A1-2. In addition to product ions at *m/z* 422, those originating from the GPI moiety were detected at *m/z* 404 (PO_4-Man-GlcN$^+$), 447 (EtN-PO_4-Man-GlcN$^+$), 650 (EtN-PO_4-(HexNAc-)Man-GlcN$^+$), 787 (peptide-EtN$^+$), 868 (peptide-EtN-PO_4^+), 1191 (peptide-EtN-PO_4-Man-Man$^+$), 1477 (peptide-EtN-PO_4-Man-Man-(EtN-PO_4-)Man$^+$), 1638 (peptide-EtN-PO_4-Man-Man-(EtN-PO_4-)Man-GlcN$^+$), and 1898 (peptide-EtN-PO_4-Man-Man-(EtN-PO_4-)Man-GlcN-inositol-PO_4^+). From these fragments, it can be deduced that this peptide is Asp106-Cys111 carrying the GPI, as indicated in the inset in Fig. 7(A).

The other GPI-peptide in peak A1-1 was characterized as having side chains; -Hex attached to M1, -PO_4-EtN and -HexNAc attached to M3, based on the product ion spectrum of the doubly charged precursor ion at *m/z* 1132 (data not shown). These two GPI structures are identical to those that have been previously reported [24].

Product ion spectra of doubly charged ion at *m/z* 1151 and 1213 suggested that they contained GPI which bear one HexNAc or two Hex in addition to GPI in Fig. 7(A) respectively. Fig. 7(B) shows the product ion spectra of the doubly charged precursor ions at *m/z* 1151 in peak A1-2. In addition to *m/z* 422, we detected product ions at *m/z* 366 (HexNAc-Man$^+$), 447 (EtN-PO_4-Man-GlcN$^+$), 650 (EtN-PO_4-(HexNAc-)Man-GlcN$^+$), 1229 (peptide-EtN-PO_4-(HexNAc-)Man$^+$), 1391 (peptide-EtN-PO_4-(HexNAc-)Man-Man$^+$), 1676 (peptide-EtN-PO_4-(HexNAc-)Man-Man-(EtN-PO_4-)Man$^+$), 1838 (peptide-EtN-PO_4-(HexNAc-)Man-Man-(EtN-PO_4-)Man-GlcN$^+$), and 1880 (peptide-EtN-PO_4-(HexNAc-)Man-Man-(EtN-PO_4-)(HexNAc-)Man$^+$). These fragment ions suggest the attachment of -HexNAc to Man1, and -PO_4-EtN and -HexNAc to Man3 as indicated in the inset of Fig. 7(B). Similarly, product ion spectra of the doubly charged precursor ion at *m/z* 1213 indicate the attachment of 2Hex and HexNAc to Man1 and Man3-PO_4-EtN (data not shown). To our knowledge, this is the first report of these two GPI structures in Thy-1.

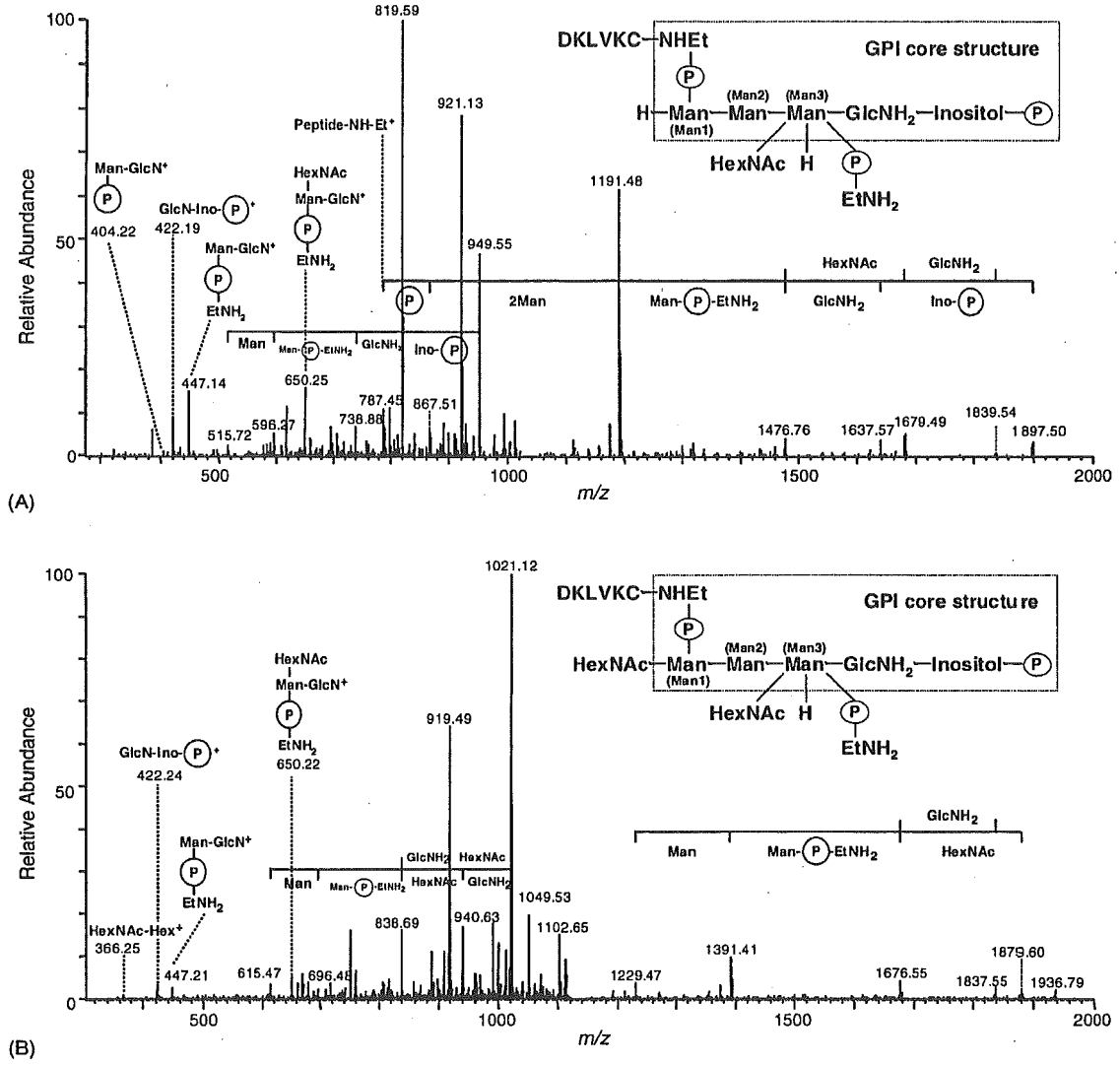

Fig. 7. Product ion spectra of the doubly charged GPI-peptide at *m/z* 1051 (A), and at *m/z* 1151 (B) in peak A1-2. The inset is the deduced structure of the GPI-peptide, and the core structure of GPI is the inside dashed line. Man, mannose; HexNAc, *N*-acetylhexosamine; $GlcNH_2$, glucosamine; $EtNH_2$-P, phosphorylethanolamine; Ino-P, inositol-phosphate.

3.5. *Analysis of Asp-N digested Thy-1*

Glycopeptides obtained by Asp-N digestion were also localized by in-source CID using marker ions at *m/z* 204 and 292 (Fig. 6(D and E)), and neutral loss of 81 u by data-dependent CID-MS/MS (Fig. 6(F)). Product ion spectra of glycopeptides were sorted by using B series ions as marker ions from those acquired around localized elution positions. Consequently, peaks A2-7 were identified as those of glycopeptides (Fig. 6(A)). The oligosaccharide structures in the glycopeptides were then characterized based on their product ion spectra (Table 1). In addition to the high-mannose-type oligosaccharides, M5, 6, and 7 deduced by LC/MS^n of tryptic digests, the oligosaccharide at Asn23 was characterized as $dHex_{0-1}Hex_{3,5,6}HexNAc_{3-5}NeuAc_{0,1}$, complex-type and hybrid-type oligosaccharides containing Lewis a/x or bisecting GlcNAc as a partial structure. Asn74 is attached by *N*-glycans with $dHex_{0-2}Hex_{3-6}HexNAc_{2,4,5}NeuAc_{0,1}$. They were high-mannose-type oligosaccharide, M5, complex-type oligosaccharides containing core Fuc and Lewis a/x as a partial structure, and hybrid-type oligosaccharides with core Fuc. Asn98 is occupied by high-mannose-type oligosaccharides, M5, and *N*-glycans with $dHex_{0-2}Hex_{3,5,6}HexNAc_{2-5}NeuAc_{0,1}$, hybrid-type oligosaccharides containing Lewis a/x or blood group H-determinant as a partial structure, which were found to be of greater diversity than those deduced by analysis of tryptic digests.

4. Discussion

In the present study, we have developed an efficient and convenient strategy for characterization, including protein identification and glycosylation analysis, of a small amount of unknown protein. We used gel electrophoresis, which is a powerful tool for separation of a small amount of protein from complex proteins mixture, especially from insoluble membrane fractions. For the complete glycosylation analysis, we examined the extraction of a whole glycoprotein from the gel, followed by trypsin digestion. Additionally, for the effective glycopeptide analysis, we studied mass spectrometric peptide/glycopeptide mapping by LC/MS^n with in-source CID and data-dependent MS^n. The glycopeptides were localized in the peptide/glycopeptide map by using oxonium ions as marker ions such as $HexNAc^+$ and $NeuAc^+$, which were generated by in-source CID, and neutral loss by data-dependent CID-MS/MS. For simultaneous identification of both peptides and glycopeptides, we conducted the database search analysis using search parameters containing a possible glycosylation at Asn with GlcNAc (203 Da). We successfully determined the sequences of peptides and some of the glycopeptides, which were localized by in-source CID and data-dependent CID-MS^n. The database search analysis using these search parameters was useful for identifying the glycopeptides resulting from predictable proteinase digestion. Glycopeptides caused by irregular digestion could be identified by assignment of peptide b and y series ions, which arose from further MS^n. The oligosaccharide structures of the identified glycopeptides were characterized on the basis of their product ion spectra. In this way, we were able to isolate rat brain Thy-1 and to elucidate *N*-glycosylation at Asn23, 74, and 98 as well as the structure of the GPIs at Cys111.

Post-translationally modified peptides could not be identified by the database search analysis. It has been particularly difficult to identify glycopeptides by database search analysis due to their complicated product ions resulting from the cleavage of glycosidic bonds. It has recently been reported that peptide + GlcNAc ion generated from a glycopeptide by CID-MS/MS yields b and y series ions by further MS^n, and that these ions can be utilized for identification of the peptide backbone and its glycosylation site [15,16,18]. Additionally, search analysis using the database including the possibility of glycosylation at Asn with all possible cleavage products of the known glycopeptides can be utilized for identification of glycopeptides in the peptide/glycopeptide map [19]. This ability would be helpful in the identification of glycoproteins whose glycosylation are already known. In the present study, we carried out a database search analysis using search parameters containing a possible glycosylation at Asn with only GlcNAc (203 Da), and successfully identified an unknown glycoprotein and *N*-glycosylated sites. This search analysis can be used for the identification of *O*-glycosylation, which has no consensus amino acid sequence, by using search parameters containing possible glycosylations at Ser/Thr with Hex, HexNAc, and dHex.

Precursor ion scans have been used for the localization the glycopeptides in peptide/glycopeptide mapping [10,11,13]. Although this method can be used for monitoring the peptides with predictable modification by setting mass of fragment ions prior to scanning, peptides with unpredictable modification cannot be detected. In contrast, in-source CID and CID-MS/MS are capable of localizing of the modified peptides after just one data acquisition using objective oxonium ions and neutral losses. In the present study, we were able to localize GPI-peptides in the peptide/glycopeptide map using EtN-PO_4-Man^+ and GlcN-Inositol-PO_4^+ generated by in-source CID [25] and to elucidate the GPI structures. We also could localize the glycopeptides with dHex, HexNAc, and NeuAc at the non-reducing ends as well as Hex using neutral loss by CID-MS/MS.

Site-specific glycosylation analysis of rat brain Thy-1 was performed after purification with monoclonal antibody affinity chromatography. Released oligosaccharides from fractionated trypsin-digested glycopeptides were analyzed by conventional analytical methods, including exoglycosidase digestion and methylation analysis [26]. In the present study, we separated PIPLC-treated GPI-anchored proteins of rat brain by SDS-PAGE, and conducted site-specific glycosylation analysis by LC/MS^n. Using a simpler step, we could elucidate the glycosylation at each glycosylation site with a greater variety of oligosaccharides than that reported previously and four GPI structures, including two novel attached structures.

Our strategy presented herein can relatively simply facilitate complete site-specific glycosylation analysis that used to require a series of complicated steps and is applicable to characterization of unknown proteins on 2-DE gel in proteomic study. Even in a mixture of multiple unknown glycoproteins, glycosylation of each glycoprotein can be determined based on the product ion spectra. Our method would be helpful for study of the alternation of glycosylation with growth, aging, and disease [27,28].

Acknowledgements

This study was supported in part by a Grant-in-Aid from the Ministry of Health, Labor and Welfare, Core Research for the Evolutional Science and Technology Program (CREST) of the Japan Science and Technology Agency (JST), and Research on Health Science focusing on Drug Innovation from The Japan Health Science Foundation (N.K.).

We appreciate Dr. A. Hachisuka of the National Institute of Health Science for her technical advice.

We would also like to thank Dr. M. Kubota and Mr. M. Yoshida of Thermo Electron K.K. (Japan), for their technical support.

References

[1] A. Varki, Glycobiology 3 (1993) 97.
[2] H. Sasaki, B. Bothner, A. Dell, M. Fukuda, J. Biol. Chem. 262 (1987) 12059.
[3] F. Wang, A. Nakouzi, R.H. Angeletti, A. Casadevall, Anal. Biochem. 314 (2003) 266.
[4] K. Hirayama, R. Yuji, N. Yamada, K. Kato, Y. Arata, I. Shimada, Anal. Chem. 70 (1998) 2718.
[5] M. Ohta, N. Kawasaki, S. Itoh, T. Hayakawa, Biologicals 30 (2002) 235.
[6] E. Mortz, T. Sareneva, S. Haebel, I. Julkunen, P. Roepstorff, Electrophoresis 17 (1996) 925.
[7] F.G. Hanisch, M. Jovanovic, J. Peter-Katalinic, Anal. Biochem. 290 (2001) 47.
[8] D. von Witzendorff, M. Ekhlasi-Hundrieser, Z. Dostalova, M. Resch, D. Rath, H.W. Michelmann, E. Topfer-Petersen, Glycobiology 15 (2005) 475.
[9] B. Küster, T.N. Krogh, E. Mortz, D.J. Harvey, Proteomics 1 (2001) 350.
[10] S.A. Carr, M.J. Huddleston, M.F. Bean, Protein Sci. 2 (1993) 183.
[11] M.J. Huddleston, M.F. Bean, S.A. Carr, Anal. Chem. 65 (1993) 877.
[12] R.S. Annan, S.A. Carr, J. Protein Chem. 16 (1997) 391.
[13] K. Sandra, I. Stals, P. Sandra, M. Claeyssens, J. Van Beeumen, B. Devreese, J. Chromatogr. A 1058 (2004) 263.
[14] A. Harazono, N. Kawasaki, T. Kawanishi, T. Hayakawa, Glycobiology 15 (2005) 447.
[15] U.M. Demelbauer, M. Zehl, A. Plematl, G. Allmaier, A. Rizzi, Rapid Commun. Mass Spectrom. 18 (2004) 1575.
[16] Y. Wada, M. Tajiri, S. Yoshida, Anal. Chem. 76 (2004) 6560.
[17] B. Sullivan, T.A. Addona, S.A. Carr, Anal. Chem. 76 (2004) 3112.
[18] S. Zhang, D. Chelius, J. Biomol. Tech. 15 (2004) 120.
[19] S. Wu, P. Bondarenko, T. Shaler, P. Shieh, W. Hancock, Thermo Finnigan LC/MS^n Application Report Application Report No. 300.
[20] C. Bordier, J. Biol. Chem. 256 (1981) 1604.
[21] M.P. Lisanti, M. Sargiacomo, L. Graeve, A.R. Saltiel, E. Rodriguez-Boulan, Proc. Natl. Acad. Sci. U.S.A. 85 (1988) 9557.
[22] S. Itoh, N. Kawasaki, M. Ohta, T. Hayakawa, J. Chromatogr. A 978 (2002) 141.
[23] B. Domon, C.E. Costello, J. Glycoconjugate 5 (1988) 397.
[24] S.W. Homans, M.A. Ferguson, R.A. Dwek, T.W. Rademacher, R. Anand, A.F. Williams, Nature 333 (1988) 269.
[25] K. Fukushima, Y. Ikehara, M. Kanai, N. Kochibe, M. Kuroki, K. Yamashita, J. Biol. Chem. 278 (2003) 36296.
[26] R.B. Parekh, A.G. Tse, R.A. Dwek, A.F. Williams, T.W. Rademacher, EMBO J. 6 (1987) 1233.
[27] Y. Sato, M. Kimura, C. Yasuda, Y. Nakano, M. Tomita, A. Kobata, T. Endo, Glycobiology 9 (1999) 655.
[28] G. Durand, N. Seta, Clin. Chem. 46 (2000) 795.

J. Biochem. **137**, 579–586 (2005)
DOI: 10.1093/jb/mvi070

Thrombomodulin Enhances the Invasive Activity of Mouse Mammary Tumor Cells

Shingo Niimi[1,*], Mizuho Harashima[2], Kazuko Takayama[2], Mayumi Hara[2], Masashi Hyuga[1], Taiichiro Seki[2], Toyohiko Ariga[2], Toru Kawanishi[1] and Takao Hayakawa[3]

[1]Division of Biological Chemistry and Biologicals, National Institute of Health Sciences, Kamiyoga 1-18-1, Setagaya-ku, Tokyo 158-8501; [2]Department of Nutrition and Physiology, Nihon University College of Bioresource Sciences, Kameino, Fujisawa 252-8510; and [3]Deputy Director General, National Institute of Health Sciences, Kamiyoga 1-18-1, Setagaya-ku, Tokyo 158-8501

Received January 31, 2005; accepted February 18, 2005

Thrombomodulin (TM) is a thrombin receptor on the surface of endothelial cells that converts thrombin from a procoagulant to an anticoagulant. Thrombin promotes invasion by various tumor cells, and positive or negative correlations are found between the expression of TM and tumorigenesis in some patients. In this study, we used an invasion assay to investigate the effect of TM on the invasive activity of a mouse mammary tumor cell line, MMT cells, and the effects of TM were compared with those of thrombin as a positive control. In the presence of 1% fetal calf serum (FCS), TM significantly stimulated MMT cell invasion in a dose-dependent manner, resulting in an approximately 3-fold increase at 1–10 pg/ml over the untreated control. Thrombin also caused a similar degree of stimulation at 50 ng/ml. Since thrombin activity was detected in the components of the assay system, an invasion assay was also performed in a thrombin-activity-depleted assay system constructed to eliminate the effect of thrombin activity; TM (10 pg/ml) plus thrombin (1 pg/ml) stimulated invasion by approximately 3.5-fold in this assay system. Hirudin, a specific thrombin inhibitor, inhibited stimulation by TM as well as by thrombin in both the presence and absence of 1% FCS. Investigations of the effects of TM on proliferation, adhesion and chemotaxis to clarify the mechanism of stimulation by TM revealed that TM does not affect proliferation or adhesion in the presence of 1% FCS, but stimulates chemotaxis by approximately 2.3-fold. Similar results were obtained in experiments using thrombin. TM (10 pg/ml) plus thrombin (1 pg/ml), on the other hand, stimulated chemotaxis by approximately 2.3-fold in the thrombin-activity-depleted assay system. Binding studies using [^{125}I]-thrombin revealed that the cells have specific saturable binding sites for thrombin. These results show that TM stimulates the invasive activity of MMT cells, probably by acting as a cofactor for the thrombin-stimulated invasion of the cells *via* its receptor and lowering the effective concentration of thrombin. The findings also indicate that the stimulation of invasive activity in the presence of 1% FCS and in the thrombin-activity-depleted assay system may mainly be mediated by the stimulation of chemotaxis.

Key words: invasion, thrombin, thrombomodulin.

Abbreviations: TM, thrombomodulin; MEM, modified Eagle's medium; CS, calf serum; FCS, fetal calf serum; MMP, matrix metalloprotease; ECM, extracellular matrix; Boc-Asp(Obzl)-pro-Arg-MCA, Boc-β-benzyl-Asp-Pro-Arg-4-methyl-coumaryl-7-amide; PBS, phosphate-buffered saline.

Thrombomodulin (TM) is a thrombin receptor on the surface of endothelial cells (*1*) that was first discovered as a cofactor for the thrombin-catalyzed activation of the anticoagulant protein C (*2*). Biologically active soluble forms of TM, which probably represent the products of limited proteolytic cleavage of cell-surface TM, were later detected in human plasma (*3*), suggesting a possible role of the soluble forms *in vivo*. TM also positively or negatively regulates various functions of thrombin as described below. TM stimulates the inactivation of pro-urokinase-type plasminogen activator (*4*), the activation of TAF I (*5*), and the activation of progelatinase A (*6*). TM inhibits the activation of platelets (*7*), the activation of factor X (*8*) and human endothelial cells (*9*), the stimulation of fibrin formation (*8*), and the proliferation of arterial smooth muscle cells (*10*) and human umbilical vein endothelial cells (*11*).

On the other hand, there are several direct and indirect lines of evidence indicating that thrombin stimulates invasion and/or metastasis by tumor cells (*12–18*), and it has recently been reported that the expression of TM is increased or decreased in some carcinomas. The expression of TM increases in squamous carcinomas of the lung (*19*), colorectal carcinomas (*20*), and some transitional

*To whom correspondence should be addressed. Tel: +81-3-3700-9347, Fax: +81-3-3700-9084, E-mail: niimi@nihs.go.jp

carcinomas (*21–22*), and its expression level is negatively correlated with the malignancy of carcinoma of the esophagus (*23*), hepatocellular carcinoma (*24*), and ovarian tumors (*25*). There is also evidence of increased serum levels of TM in some tumors, including pancreatic cancer (*26*), digestive tract carcinoma (*27*), and glioblastoma (*28*). Based on this evidence, it is likely that TM plays some role in the regulation of tumor metastasis.

In this study, we investigated the effects of TM on the invasive activity of a mouse mammary tumor cell line, MMT, by an *in vitro* invasion assay, because tumor cell invasion through the basement membrane is a critical step in the process of metastasis (*29–30*). We also compared the effects of TM with those of thrombin as a positive control.

MATERIALS AND METHODS

Materials—TM was a kind gift of Asahi Kasei Pharma, Japan. The TM was prepared as described by Gomi *et al.* (*31*). Plasmids containing the cDNA encoding TM (residues 1–498) were transfected into COS-1 cells, and the recombinant TM was purified from serum-free COS-1-cell-conditioned medium. The purified TM yielded a single band at 90 kDa in SDS-PAGE under reducing conditions. The recombinant TM was confirmed to be thrombin-free by a protein C activating assay developed in our laboratory (*32*). Thrombin (1,140 units/mg protein) was a kind gift of Mochida Pharmaceutical Co., Ltd., Japan. Hirudin was purchased from Wako (Osaka, Japan). A fluorogenic substrate, Boc-β-benzyl-Asp-Pro-Arg-4-methyl-coumaryl-7-amide (Boc-Asp(Obzl)-pro-Arg-MCA), was purchased from Peptide Institute, Inc. (Osaka, Japan).

Cell Culture—MMT mouse mammary tumor cells were obtained from the Japanese Health Science Research Resource Bank and cultured in modified Eagle's medium (MEM) supplemented with 10% calf serum (CS) on 60-mm diameter culture dishes, 4×10^5 cells per dish. After 7 d, the subconfluent MMT cells were detached from the culture dishes with 0.25% trypsin/EDTA, treated with MEM containing 10% CS, and collected by centrifugation. The cells were then washed with MEM and used in experiments. In some experiments, the thrombin activity associated with cells was depleted as described below, and the resultant cells were used for various experiments in which MEM containing 0.1% BSA was used as the basal medium. We refer to this assay system as the thrombin-activity-depleted assay system below. To deplete thrombin activity, the cell suspension (1.5×10^5 cells in 10 ml of MEM) was incubated in a non-adherent form on 100-mm diameter non-treated culture dishes pre-coated with BSA (10 mg/ml) for 2 h in a humidified chamber at 37°C under 5% CO_2, and then washed with MEM.

In Vitro Invasion Assay—In vitro invasion by MMT cells was measured in a Matrigel invasion chamber (Collaborative Biomedical Products, Bedford, MA, USA). The chamber (upper compartment) was placed in a 24-well culture plate (lower compartment), and the cell suspension (1.6×10^5 cells in 500 μl) and the basal medium (750 μl) containing various factors were added to the upper and lower compartments, respectively. MEM containing 1% fetal calf serum (FCS) or 0.1% BSA was used as the basal medium. Matrigel invasion chambers were precoated with fibronectin as described below before use in the thrombin-activity-depleted assay system. Human plasma fibronectin solution (IWAKI, Japan) was diluted to a final concentration of 5 μg/ml with phosphate-buffered saline (PBS), and a 300 μl aliquot was added to the chamber and a 750 μl aliquot to the 24-well culture plate. The chamber and 24-well plate were allowed to stand at 37°C for 2 h and were then washed with PBS. After incubating the cells for 18 h, the filters were fixed with methanol and stained with hematoxylin and eosin. The cells on the upper surface of the filters were removed by wiping with cotton swabs, and the number of cells that had migrated to the lower surface of the filters was counted under a microscope.

Measurement of Thrombin Activity—Thrombin activity in FCS, CS, and on cells was measured by the method of Kawabata *et al.* (*33*). A 10 μl volume of 10% FCS or CS was mixed with 90 μl of reaction buffer containing 50 mM Tris-HCl, pH 8.0, 100 mM NaCl, and 10 mM $CaCl_2$, with or without hirudin (0.5 unit/ml). Packed cells (1×10^6 cells) were suspended in 100 μl of reaction buffer with or without hirudin (0.5 unit/ml). After adding 1 μl of 10 mM substrate, Boc-Asp(Obzl)-pro-Arg-MCA solution to the cell suspension, the mixture was incubated for 20 min at 37°C, and the reaction was stopped by adding 600 μl of 0.6 M acetic acid. The fluorescence of the aminomethylcoumarine released was measured with a fluorospectrophotometer at an excitation wavelength of 380 nm and an emission of 460 nm. A blank solution was prepared by adding 1 μl of substrate solution to the reaction buffer mixed with 600 μl of 0.6 M acetic acid. Thrombin activity was calculated using 1, 2.5, 5 and 10 ng/ml thrombin solutions as standards and subtracting the fluorescence obtained in the presence of hirudin from that in the absence of hirudin. A linear dose-response curve was obtained between 0.5–5 ng/ml of thrombin, and its activity was inhibited by more than 98% by hirudin (0.5 unit/ml). The fluorescence of each sample was within the linear range.

Proliferation Assay—The cell suspension (1×10^5 cells in 4 ml) was seeded on 60-mm diameter culture dishes and incubated with each factor for 18 h. MEM containing 1% FCS was used as the basal medium. The cells were then detached from the culture dishes with 0.25% trypsin/EDTA, treated with MEM containing 10% CS, collected by centrifugation, and counted with a hemocytometer.

Adhesion Assay—Adhesion assays were performed by a modification of the method of Deryugina *et al.* (*34*). A 300 μl aliquot of fibronectin (5 μg/ml), prepared as described above, was added to each well of 24-well plates (IWAKI, Japan). The plates were allowed to stand overnight at 4°C, washed with PBS, blocked with 1% BSA in PBS for 1 h at 37°C, and finally washed in PBS. MMT cells (55×10^4 cells) were exposed to each factor in 2 ml of MEM containing 1% FCS for 30 min at 37°C. After washing with 2 ml of MEM, the cell suspensions (1×10^5 cells in 0.38 ml of MEM) were seeded on each well. After incubation for 30 min at 37°C, non-adherent cells were removed by washing with PBS, and the adherent cells were fixed and stained with 0.2% crystal violet in 10% ethanol for 10 min. After three washes with 2 ml of PBS,

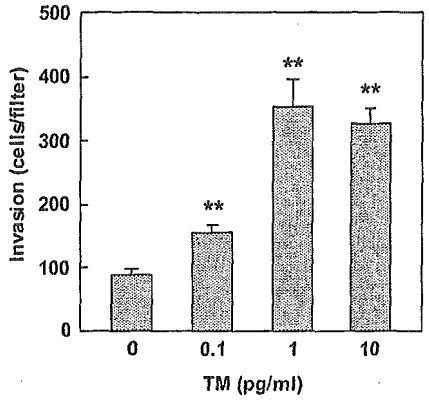

Fig. 1. **Dose dependency of the effect of TM on invasiveness.** MEM containing 1% FCS was used as the basal medium. The concentrations of TM indicated are the concentrations in the lower compartment. The data shown are means ± SD of the data obtained in duplicate wells in three experiments (**$p < 0.01$ *vs.* control). The deviation in each experiment was less than 10%.

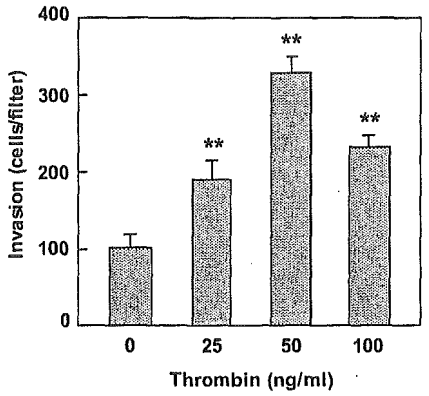

Fig. 2. **Dose dependency of the effect of thrombin on invasiveness.** MEM containing 1% FCS was used as the basal medium. The concentrations of thrombin indicated are the concentrations in the lower compartment. The data shown are means ± SD of data obtained in duplicate wells in three experiments (**$p < 0.01$ *vs.* control). The deviation in each experiment was less than 10%.

the dye was extracted in an end-over-end mixer with 600 μl of 50% ethanol in 50 mM sodium phosphate (pH 4.5) for 10 min, and absorbance was measured at 540 nm. The correlation between absorbance and cell number was confirmed in a preliminary experiment.

Chemotaxis Assay—Chemotaxis assays were performed with control inserts (Collaborative Biomedical Products, Bedford, MA, USA) in a similar manner to the invasion assay described above. The control inserts were not coated with Matrigel. MEM containing 1% FCS was used as the basal medium. The control inserts were pre-coated with fibronectin (5 μg/ml) as described for the pre-coating of the Matrigel invasion chamber in the thrombin-activity-depleted assay system.

Iodination of Thrombin and Determination of Binding—Thrombin was iodinated to a specific activity of 19.1 × 10^7 cpm/μg by the chloramine T method as described previously (*35–36*). After precoating 24-well plates with fibronectin (5 μg/ml) as described above, the cell suspensions (1.22 × 10^5 cells in 0.45 ml of MEM) were seeded into each well and incubated in a humidified chamber at 37°C under 5% CO_2 for 2 h. The cells were then washed with 0.4 ml of MEM containing 15 mM Hepes (pH 7.2) and 0.1% BSA and incubated for 1.5 h at 37°C in the same buffer with various concentrations of [^{125}I]-thrombin in the presence or absence of a 100-fold excess amount of unlabeled thrombin. After washing the cells four times with the same ice-cold buffer, the cells were solubilized with 0.4 ml of 1 N NaOH for 1 h at 37°C. Specific binding was calculated as the difference between total binding and nonspecific binding.

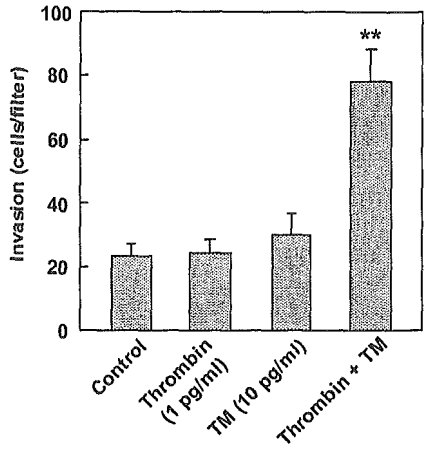

Fig. 3. **Effect of TM and thrombin on invasiveness in the thrombin-activity-depleted assay system.** Cells on which thrombin activity was depleted were used in the experiment. MEM containing 0.1% BSA was used as the basal medium. The data shown are means ± SD of data obtained in duplicate wells in three experiments (**$p < 0.01$ *vs. control*). The deviation in each experiment was less than 10%.

RESULTS

Effect of TM on Invasiveness—Figure 1 shows the effects of TM on the invasive activity of MMT cells in the presence of 1% FCS. TM significantly stimulated invasive activity in a dose-dependent manner, resulting in an approximately 3-fold stimulation at 1–10 pg/ml. Figure 2 shows the effects of thrombin used as a positive control. Thrombin also stimulated invasive activity in a dose-dependent manner.

On the basis of these findings, we investigated the possibility that the stimulation of invasion by TM might be dependent on thrombin that may have been introduced into the assay system as described below. First, thrombin activity in the assay system was measured. The thrombin concentrations in freshly prepared 10% FCS and CS measured by the thrombin activity assay were 200 pg/ml and 2.8 ng/ml, respectively. The amount of thrombin on the cells measured in a similar manner was 35 pg/10^6 cells. Based on these values, the thrombin concentrations in the assay system with or without 1% FCS were estimated to be 24.48 and 4.48 pg/ml, respectively. Second, the action of TM was examined in the thrombin-activity-depleted assay system described in "MATERIALS AND METHODS," and depletion of thrombin activity in the

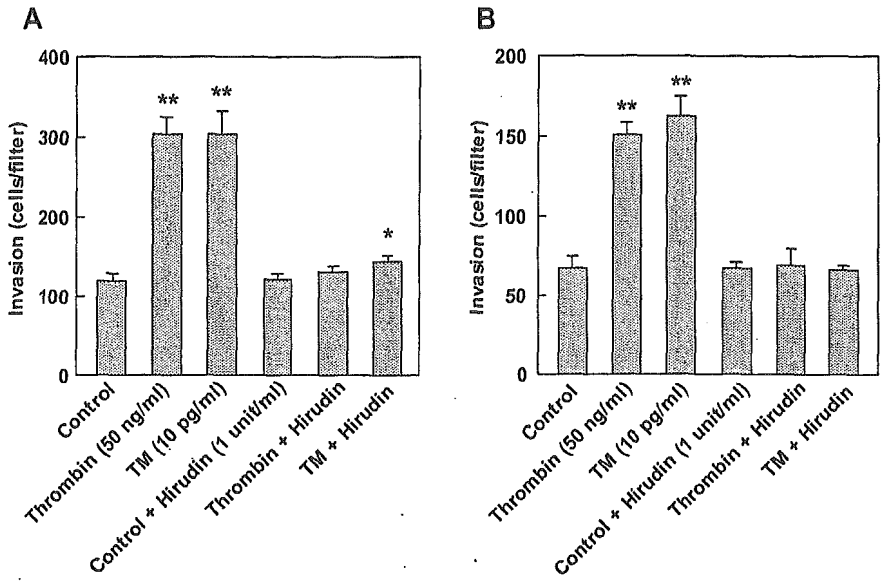

Fig. 4. **Effect of hirudin on the stimulation of invasion by TM.** (A) MEM containing 1% FCS was used as the basal medium. The indicated concentration of each factor is that in the lower compartment. The data shown are means ± SD of data obtained in duplicate wells in three experiments (*$p < 0.05$ *vs.* control; **$p < 0.01$ *vs.* control) (B) MEM containing 0.1% BSA was used as the basal medium. The data shown are means ± SD of data obtained in duplicate wells in three experiments (**$p < 0.01$ *vs.* control). The deviation in each experiment was less than 10%.

assay system was confirmed by the absence of any detectable thrombin activity on the cells. Figure 3 shows the effects of thrombin (1 pg/ml) and TM (10 pg/ml) on the invasive activity of cells in the thrombin-activity-depleted assay system. While neither thrombin or TM had any effect on invasion, TM plus thrombin stimulated invasion by approximately 3-fold.

Effect of Hirudin on the Stimulation of Invasion by TM—The action of TM was also examined in the presence of the specific thrombin inhibitor hirudin to investigate the possibility described above. Fig. 4, A and B, shows the effects of hirudin on the invasion-stimulating activity of TM in the presence and absence of 1% FCS. We used a 1 unit/ml concentration of hirudin in this experiment, because 50 ng/ml thrombin corresponds to 0.057 unit/ml, and so 1 unit/ml hirudin seemed adequate to inhibit this concentration of thrombin. As expected, hirudin (1 unit/ml) not only inhibited the stimulation by thrombin to control levels, but the stimulation by TM as well.

Effect of TM on Proliferation—Since tumor cell invasion consists of a series of events, including adhesion to the extracellular matrix (ECM) and chemotaxis, we investigated the effects of TM on these two events to clarify the molecular mechanism of the stimulation of invasive activity by TM. Before investigating the effect of TM on these processes, we investigated its effects on cell proliferation to confirm that the stimulation of invasive activity by TM is not an artifact of the enhancement of cell proliferation.

Figure 5 shows the effects of TM on MMT cell proliferation in the presence of 1% FCS. The numbers of cells in the presence of TM or thrombin did not differ from the numbers in the control cultures.

Effect of TM on Adhesion to Fibronectin—Figure 6 shows the effects of TM on adhesion to fibronectin, a basal lam-

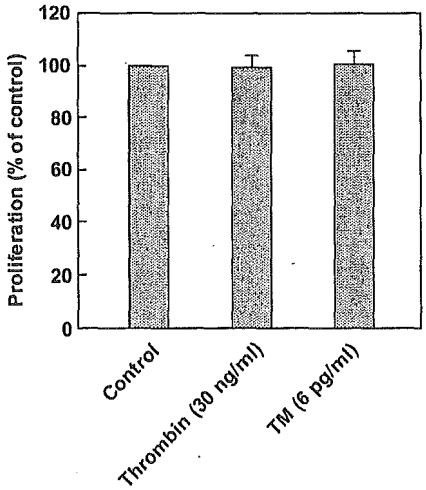

Fig. 5. **Effect of TM on proliferation.** MEM containing 1% FCS was used as the basal medium. The data shown are means ± SD of data obtained in duplicate dishes in three experiments. The deviation in each experiment was less than 10%.

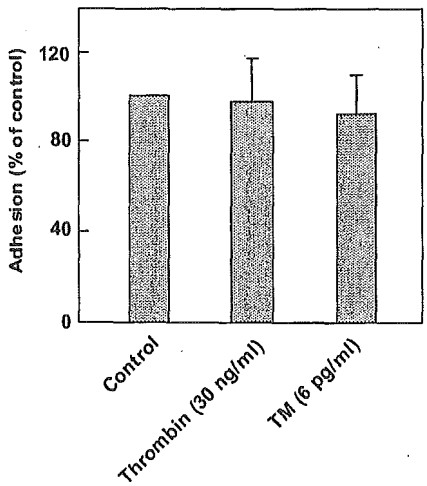

Fig. 6. **Effect of TM on adhesion to fibronectin.** MEM containing 1% FCS was used as the basal medium. The data shown are means ± SD of data obtained in duplicate wells in three experiments. The deviation in each experiment was less than 10%.

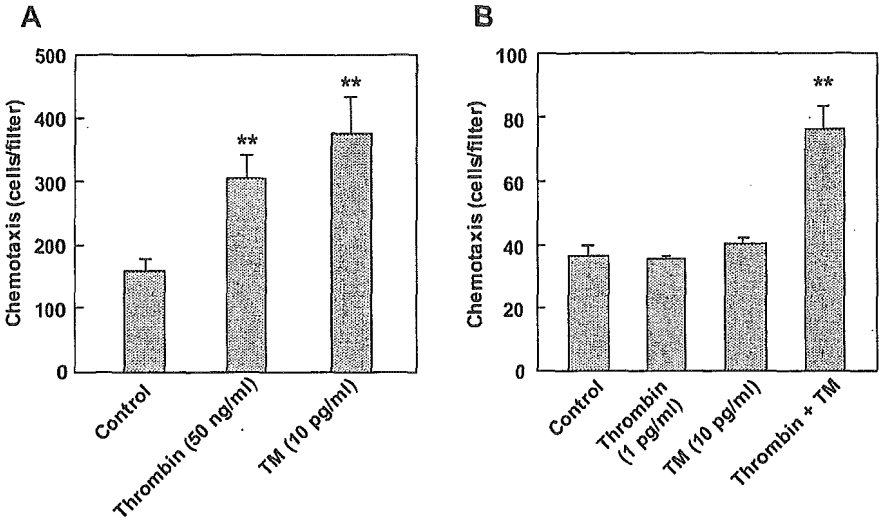

Fig. 7. **Effect of TM on chemotaxis.** (A) MEM containing 1% FCS was used as the basal medium. The data shown are means ± SD of data obtained in duplicate wells in three experiments (**$p < 0.01$ *vs.* control). (B) Cells on which thrombin activity was depleted were used in the experiment. MEM containing 0.1% BSA was used as the basal medium. The data shown are means ± SD of data obtained in duplicate wells in three experiments (**$p < 0.01$ *vs.* control). The deviation in each experiment was less than 10%.

ina component. Neither TM nor thrombin affected adhesion to fibronectin.

Effect of TM on Chemotaxis—Figure 7 (A and B), shows the effects of TM on chemotaxis by MMT cells in the presence of 1% FCS and in the thrombin-activity-depleted assay system, respectively. Both TM (10 pg/ml) and thrombin (50 ng/ml) significantly stimulated chemotaxis by MMT cells by approximately 1.9–2.3-fold in the former system, but neither TM (10 pg/ml) nor thrombin (1 pg/ml) affected chemotaxis in the latter system; TM plus thrombin, on the other hand, stimulated chemotaxis by approximately 2-fold.

Binding of Thrombin—Figure 8 shows the binding curves for specific [^{125}I]-thrombin binding sites on cells in the presence and absence of TM (10 pg/ml). These binding curves show the specific [^{125}I]-thrombin binding to be saturable at approximately 40 ng/ml, and that TM has no effect on the specific binding of [^{125}I]-thrombin. A similar binding experiment was performed in the [^{125}I]-thrombin concentration range of 1–10 pg/ml, but no specific binding was detected independent of the presence or absence of TM, probably because the absolute amount of radioactivity used was too low to be detected as specific binding.

DISCUSSION

In the present study, we show that, at its maximum effective dose, TM stimulates the invasive activity of MMT cells *in vitro* by approximately 3-fold. As far as we know, this is the first time that TM has been shown to stimulate the invasive activity of tumor cells *in vitro*. Similarly, exogenous thrombin causes maximal stimulation of invasion at 50 ng/ml, which is a concentration more than 1,000-fold higher than the maximum effective dose of TM.

Since TM acts as a cofactor for the thrombin-catalyzed activation of protein C and increases the rate of the reaction by >1,000-fold (*8*), the stimulation by TM may have been due to TM interacting with thrombin, which had been introduced into the assay system, and acting as a cofactor for thrombin-stimulated invasion of MMT cells, thus lowering the effective concentration of thrombin. This possibility seems to be supported by the detection of thrombin activity in the assay systems, the requirement for thrombin for stimulation by TM in the thrombin-activity-depleted assay system, and the inhibition of stimulation by hirudin. It is noteworthy that the thrombin concentration required for stimulation by TM in the thrombin-activity-depleted assay system is more than 20,000-fold less than the concentration required for thrombin to stimulate invasion. On the other hand, the control level was not inhibited by hirudin in the presence of 1% FCS, probably due to the lower thrombin concentration in the assay system compared with the effective concentration of exogenous thrombin.

There have been two studies examining the effect of TM on the invasive activity of tumor cells. Matsushita *et al.* showed that a subcloned human esophageal squamous cell carcinoma line with low TM expression is more invasive than a high TM-expressing clone (*37*). In their study, the action of TM does not seem to be due to an acceleration of its thrombin cofactor activity, because the difference between the cell lines with low and high TM expression with respect to their cofactor activity for protein C activation by thrombin was less than 13% and significantly lower than their TM levels and invasive activities. Hosaka *et al.* showed that TM (10–100 ng/ml)

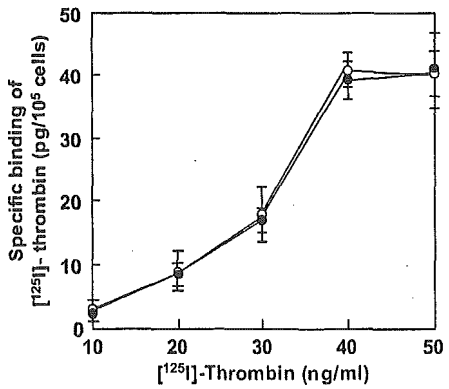

Fig. 8. **Binding of [^{125}I]-thrombin.** Specific binding of [^{125}I]-thrombin to cells in the absence (solid circles) and presence of TM (10 pg/ml) (open circles) was measured. The data shown are representative specific binding curves for [^{125}I]-thrombin binding sites and are means ± SD of data obtained in triplicate wells.

inhibits the invasive activity of mouse melanoma cells *in vitro* (*38*), and TM has also been found to decrease the proliferation of tumor cell lines subcloned from patients with malignant melanomas (*39*). None of these inhibitory effects were inhibited by hirudin.

In contrast to these studies, the present study shows that TM enhances the invasive activity of MMT cells and indicates that the action of TM is entirely dependent on thrombin as described above. Therefore, the mode and mechanism of action of TM in MMT cells seems to be different from its mode and mechanism of action in the squamous cell carcinoma line and melanoma cells.

It is useful to speculate on the role of TM in tumorigenesis based on the findings of our study, because tumor cell invasion through the basement membrane is a critical step in the process of metastasis (*29–30*). Several studies have shown that TM levels in serum increase in patients with certain tumors (*26–28*), as described in the Introduction. Thus, the results of this study suggest that the soluble form of TM may play a positive role in the malignancy of some kinds of tumors, probably by enhancing the metastatic potential of thrombin. On the other hand, TM on the cell surface may act as a negative regulator to thrombin, because thrombin is degraded as the thrombin-TM complex by its internalization after binding to TM on the cell surface (*40*). This possibility may be supported by the findings that the expression level of TM is negatively correlated with the malignancy of some carcinomas (*23–25*), as described in the Introduction.

Tumor cell invasion is a complex process that involves adhesion to ECM, degradation of ECM, and chemotaxis (*41*). Chemotaxis is the essential step in invasion as reviewed by Wells (*42*). The results of the present study show that both TM and thrombin stimulate chemotaxis in the presence of 1% FCS, and that TM plus thrombin stimulate chemotaxis in the thrombin-activity-depleted assay system. Both of these findings are consistent with previous reports that thrombin stimulates chemotaxis (*17, 18*), and the presence of specific binding sites for thrombin on cells indicates that these actions are mediated by thrombin receptors.

However, other actions of thrombin may also be involved in the stimulation of tumor cell invasion, because the enhancement of chemotaxis alone is insufficient to account for the increase in tumor cell invasion. One such other possible action of thrombin is the stimulation of the matrix metalloprotease (MMP)–mediated degradation of a variety of ECM proteins, including collagens type IV, V, VII, and X, fibronectin, laminin (*43–47*), elastin (*48–49*), proteoglycans (*49–51*), and entactin (*52*). Several reports have indicated that thrombin increases the active forms of MMP-2 and MMP-9 (*53–59*), and plays important roles in the enhancement of tumor cell invasion and metastasis (*34, 60–68*). There are also reports that thrombin stimulates the release of MMP-2 (*69*), the expression of MMP-1 and MMP-3 (*70*), and the expression of MMP-9 mRNA (*71*). Another possible action is the stimulation of MMP-independent degradation of ECM. This possibility appears to be supported by the finding that thrombin stimulates the expression of urokinase-type plasminogen activator, a factor involved in the degradation of ECM protein (*72*), and stimulates the heparinase-mediated release of heparan sulfate from ECM (*73*).

In conclusion, the results of this study show that TM stimulates the invasive activity of MMT cells, probably by acting as a cofactor for the thrombin-stimulated invasion of cells mediated by thrombin receptors, and by lowering the effective concentration of thrombin. Further, the results indicate that the stimulation is mainly caused by an enhancement of chemotaxis.

This study was supported, in part, by a Grant-in-Aid for research on health sciences focusing on drug innovation from the Japan Health Sciences Foundation.

REFERENCES

1. Esmon, C.T. and Owen, W.G. (1981) Identification of an endothelial cell cofactor for thrombin-catalyzed activation of protein C. *Proc. Natl Acad. Sci. USA* **78**, 2249–2252
2. Esmon, C.T. (1989) The roles of protein C and thrombomodulin in the regulation of blood coagulation. *J. Biol. Chem.* **264**, 4743–4746
3. Ishii, H. and Majerus, P.W. (1985) Thrombomodulin is present in human plasma and urine. *J. Clin. Invest.* **76**, 2178–2181
4. Molinari, A., Giorgetti, C., Lansen, J., Vaghi, F., Orsini, G., Faioni, E.M., and Mannucci, P.M. (1992) Thrombomodulin is a cofactor for thrombin degradation of recombinant single-chain urokinase plasminogen activator "in vitro" and in a perfused rabbit heart model. *Thromb. Haemost.* **67**, 226–232
5. Bajzar, L., Morser, J., and Nesheim, M. (1996) TAFI, or plasma procarboxypeptidase B, couples the coagulation and fibrinolytic cascades through the thrombin-thrombomodulin complex. *J. Biol. Chem.* **271**, 16603–16608
6. Pekovich, S.R., Bock, P.E., and Hoover, R.L. (2001) Thrombin-thrombomodulin activation of protein C facilitates the activation of progelatinase A. *FEBS Lett.* **494**, 129–132
7. Esmon, N.L., Carroll, R.C., and Esmon, C.T. (1986) Thrombomodulin blocks the ability of thrombin to activate platelets. *J. Biol. Chem.* **258**, 12238–12242
8. Esmon, C.T., Esmon, N.L., and Harris, K.W. (1983) Complex formation between thrombin and thrombomodulin inhibits both thrombin-catalyzed fibrin formation and factor V activation. *J. Biol. Chem.* **257**, 7944–7947
9. Parkinson, J.F., Bang, N.U., and Garcia, J.G. (1993) Recombinant human thrombomodulin attenuates human endothelial cell activation by human thrombin. *Arterioscler. Thromb.* **13**, 1119–1123
10. Li, J., Garnette, C.S., Cahn, M., Claytor, R.B., Rohrer, M.J., Dobson, J.G. Jr., Gerlitz. B., and Cutler, B.S. (2000) Recombinant thrombomodulin inhibits arterial smooth muscle cell proliferation induced by thrombin. *J. Vasc. Surg.* **32**, 804–813
11. Lafay, M., Laguna, R., Le Bonniec, B.F., Lasne, D., Aiach, M., and Rendu, F. (1998) Thrombomodulin modulates the mitogenic response to thrombin of human umbilical vein endothelial cells. *Thromb. Haemost.* **79**, 848–852
12. Nierodzik, M.L., Plotkin, A., Kajumo, F., and Karpatkin, S. (1991) Thrombin stimulates tumor-platelet adhesion *in vitro* and metastasis *in vivo*. *J. Clin. Invest.* **87**, 229–236
13. Nierodzik, M.L., Kajumo, F., and Karpatkin, S. (1992) Effect of thrombin treatment of tumor cells on adhesion of tumor cells to platelets *in vitro* and tumor metastasis *in vivo*. *Cancer Res.* **52**, 3267–3272
14. Esumi, N., Fan, D., and Fidler, J.I. (1991) Inhibition of murine melanoma experimental metastasis by recombinant desulfatohirudin, a highly specific thrombin inhibitor. *Cancer Res.* **51**, 4549–4556
15. Wojtukiewicz, M.Z., Tang, D.G., Ben-Josef, E., Renaud, C., Walz, D.A., and Honn, K.V. (1995) Solid tumor cells express functional 'tethered ligand' thrombin receptor. *Cancer Res.* **55**, 698–704
16. Even-Ram, S., Uziely. B., Cohen, P., Grisaru-Granovsky, S., Maoz, M., Ginzburg, Y., Reich, R., Vlodavsky, I., and Bar-

Shavit, R. (1998) Thrombin receptor overexpression in malignant and physiological invasion processes. *Nat. Med.* **4**, 909–914
17. Hernandez-Rodriguez, N.A., Correa, E., Contreras-Paredes, A., and Green, L. (1999) Evidence that thrombin present in lungs of patients with pulmonary metastasis may contribute to the development of the disease. *Lung Cancer* **26**, 157–167
18. Henrikson, K.P., Salazar, S.L., Fenton, J.W. II., and Pentecost, B.T. (1999) Role of thrombin receptor in breast cancer invasiveness. *Br. J. Cancer* **79**, 401–406
19. Ogawa, H., Yonezawa, S., Maruyama, I., Matsushita, Y., Tezuka, Y., Toyoyama, H., Yanagi, M., Matsumoto, H., Nishijima, H., Shimotakahara, T., Aikou, T., and Sato, E. (2000) Expression of thrombomodulin in squamous cell carcinoma of the lungs: its relationship to lymph node metastasis and prognosis of the patients. *Cancer Lett.* **149**, 95–103
20. Takebayashi, Y., Yamada, K., Maruyama, I., Fujii, R., Akiyama, S., and Aikou, T. (1995) The expression of thymidine phosphorylase and thrombomodulin in human colorectal carcinomas. *Cancer Lett.* **92**, 1–7
21. Ordonez, N.G. (1997) Value of thrombomodulin immunostaining in the diagnosis of transitional cell carcinoma: a comparative study with carcinoembryonic antigen. *Histopathology* **31**, 517–524
22. Ordonez, N.G. (1998) Thrombomodulin expression in transitional cell carcinoma. *Am. J. Clin. Pathol.* **110**, 385–390
23. Matsumoto, M., Natsugoe, S., Nakashima, S., Shimada, M., Nakano, S., Kusano, C., Baba, M., Takao, S., Matsushita, Y., and Aikou, T. (2000) Biological evaluation of undifferentiated carcinoma of the esophagus. *Ann. Surg. Oncol.* **7**, 204–209
24. Suehiro, T., Shimada, M., Matsumata, T., Taketomi, A., Yamamoto, K., and Sugimachi, K. (1995) Thrombomodulin inhibits intrahepatic spread in human hepatocellular carcinoma. *Hepatology* **21**, 1285–1290
25. Wilhelm, S., Schmitt, M., Parkinson, J., Kuhn, W., Graeff, H., and Wilhelm O.G. (1998) Thrombomodulin, a receptor for the serine protease thrombin, is decreased in primary tumors and metastases but increased in ascitic fluids of patients with advanced ovarian cancer FIGO IIIc. *Int. J. Oncol.* **13**, 645–651
26. Lindahl, A.K., Boffa, M.C., and Abildgaard, U. (1993) Increased plasma thrombomodulin in cancer patients. *Thromb. Haemost.* **69**, 112–114
27. Boffa, M.C., Lapeyrere, C., Berard, M., Lindahl, A.K., Flageul, B., Chemaly, P., Abildgaard, U., and Dubertret, L. (1994) Plasma thrombomodulin level in malignancy varies according to the tumor type. *Nouv. Rev. Fr. Hematol.* **36**, S87–88
28. Salmaggi, A., Eoli, M., Frigerio, S., Ciusani, E., Silvani, A., and Boiardi, A. (1999) Circulating intercellular adhesion molecule-1 (ICAM-1), vascular cell adhesion molecule-1 (VCAM-1) and plasma thrombomodulin levels in glioblastoma patients. *Cancer Lett.* **146**, 169–172
29. Liotta, L.A. (1986) Tumor invasion and metastases-role of the extracellular matrix: Rhoads Memorial Award lecture. *Cancer Res.* **46**, 1–7
30. Terranova, V.P., Hujanen, E.S., and Martin, G.R. (1986) Basement membrane and the invasive activity of metastatic tumor cells. *J. Natl Cancer Inst.* **77**, 311–316
31. Gomi, K., Zushi, M., Honda, G., Kawahara, S., Matsuzaki, O., Jr., Kanabayashi, T., Yamamoto, S., Maruyama, I., and Suzuki, K. (1990) Antithrombotic effect of recombinant human thrombomodulin on thrombin-induced thromboembolism in mice. *Blood* **75**, 1396–1399
32. Niimi, S., Oshizawa, T., Naotsuka, M., Ohba, S., Yokozawa, A., Murata, T., and Hayakawa, T. (2002) Establishment of a standard assay method for human thrombomodulin and determination of the activity of the Japanese reference standard. *Biologicals* **30**, 69–76
33. Kawabata, S., Miura, T., Morita, T., Kato, H., Fujikawa, K., Iwanaga, S., Takada, K., Kimura, T., and Sakakibara, S. (1988) Highly sensitive peptide-4-methylcoumaryl-7-amide substrates for blood-clotting proteases and trypsin. *Eur. J. Biochem.* **172**, 17–25
34. Deryugina, E.I., Luo, G.X., Reisfeld, R.A., Bourdon, M.A., and Strongin, A. (1997) Tumor cell invasion through matrigel is regulated by activated matrix metalloproteinase-2. *Anticancer Res.* **17**, 3201–3210
35. Greenwood, F.C., Hunter, W.M., Glover, J.S. (1963) The preparation of ^{131}I-labelled human growth hormone of high specific radioactivity. *Biochem. J.* **89**, 114–123
36. Haeuptle, M.T., Aubert, M.L., Djiane J., Kraehenbuhl, J.P. (1983) Binding sites for lactogenic and somatogenic hormones from rabbit mammary gland and liver. *J. Biol. Chem.* **258**, 305–314
37. Matsushita, Y., Yoshiie, K., Imamura, Y., Ogawa, H., Imamura, H., Takao, S., Yonezawa, S., Aikou, T., Maruyama, I., and Sato, E. (1998) A subcloned human esophageal squamous cell carcinoma cell line with low thrombomodulin expression showed increased invasiveness compared with a high thrombomodulin-expressing clone—thrombomodulin as a possible candidate for an adhesion molecule of squamous cell carcinoma. *Cancer Lett.* **127**, 195–201
38. Hosaka, Y., Higuchi, T., Tsumagari, M., and Ishii, H. (2000) Inhibition of invasion and experimental metastasis of murine melanoma cells by human soluble thrombomodulin. *Cancer Lett.* **161**, 231–240
39. Zhang, Y., Weiler-Guettler, H., Chen, J., Wilhelm, O., Deng, Y., Qiu, F., Nakagawa, K., Klevesath, M., Wilhelm, S., Bohrer, H., Nakagawa, M., Graeff, H., Martin, E., Stern, D.M., Rosenberg, R.D., Ziegler, R., and Nawroth, P.P. (1998) Thrombomodulin modulates growth of tumor cells independent of its anticoagulant activity. *J. Clin. Invest.* **101**, 1301–1309
40. Maruyama, I. and Majerus, P.W. (1985) The turnover of thrombin-thrombomodulin complex in cultured human umbilical vein endothelial cells and A549 lung cancer cells. Endocytosis and degradation of thrombin. *J. Biol. Chem.* **260**, 15432–15438
41. Hart, I.R., Goode, N.T., and Wilson, R.E. (1989) Molecular aspects of the metastatic cascade. *Biochim. Biophys. Acta* **989**, 65–84
42. Wells, A. (2000) Tumor invasion: role of growth factor-induced cell motility. *Adv. Cancer Res.* **78**, 31–101
43. Matrisian, L.M. (1990) Metalloproteinases and their inhibitors in matrix remodeling. *Ternds Genet.* **6**, 121–125
44. Collier, I.E., Wilhelm, S.M., Eisen, A.Z., Marmer, B.L., Grant, G.A., Seltzer. J.L., Kronberger, A., He. C.S., Bauer, E.A., and Goldberg, G.I. (1988) H-ras oncogene-transformed human bronchial epithelial cells (TBE-1) secrete a single metalloprotease capable of degrading basement membrane collagen. *J. Biol. Chem.* **263**, 6579–6587
45. Wilhelm, S.M., Collier, I.E., Marmer, B.L., Eisen, A.Z., Grant, G.A., and Goldberg, G.I. (1989) SV40-transformed human lung fibroblasts secrete a 92-kDa type IV collagenase which is identical to that secreted by normal human macrophages. *J. Biol. Chem.* **264**, 17213–17221
46. Fessler, L.I., Duncan, K.G., Fessler, J.H., Salo, T., and Tryggvason, K. (1984) Identification of the procollagen IV cleavage products produced by a specific tumor collagenase. *J. Biol. Chem.* **259**, 9783–9789
47. Woessner, J.F. Jr. (1991) Matrix metalloproteinases and their inhibitors in connective tissue remodeling. *FASEB J.* **5**, 2145–2154
48. Senior, R.M., Griffin, G.L., Fliszar, C.J., Shapiro, S.D., Goldberg, G.I., and Welgus, H.G. (1991) Human 92- and 72-kilodalton type IV collagenases are elastases. *J. Biol. Chem.* **266**, 7870–7875
49. Murphy, G., Cockett, M.I., Ward, R.V., and Docherty, A.J. (1991) Matrix metalloproteinase degradation of elastin, type IV collagen and proteoglycan. A quantitive comparison of the activities of 95 kDa and 72 kDa gelatinases, stromelysins-1 and -2 and punctuated metalloproteinae (PUMP). *Biochem. J.* **277**, 277–279
50. Nguyen, Q., Murphy, G., Hughes, C.E., Mort, J.S., and Roughley, P.J. (1993) Matrix metalloproteinases cleave at two distinct sites on human cartilage link protein. *Biochem. J.* **295**, 595–598

51. Fosang, A.J., Last, K., Knauper, V., Neame, P.J., Murphy, G., Hardingham, T.E., Tschesche, H., and Hamilton, J.A. (1993) Fibroblast and neutrophil collagenases cleave at two sites in the cartilage aggrecan interglobular domain. *Biochem. J.* **295**, 273–276
52. Sires, U.I., Griffin, G.L., Broekelmann, T.J., Mecham, R.P., Murphy, G., Chung, A.E., Welgus, H.G., and Senior, R.M. (1993) Degradation of entactin by matrix metalloproteinases. Susceptibility to matrilysin and identification of cleavage sites. *J. Biol. Chem.* **268**, 2069–2074
53. Zucker, S., Conner, C., DiMassmo, B.I., Ende, H., Drews, M., Seiki, M., and Bahou, W.F. (1995) Thrombin induces the activation of progelatinase A in vascular endothelial cells. Physiologic regulation of angiogenesis. *J. Biol. Chem.* **270**, 23730–23738
54. Galis, Z.S., Kranzhofer, R., Fenton, J.W. II., and Libby, P. (1997) Thrombin promotes activation of matrix metalloproteinase-2 produced by cultured vascular smooth muscle cells. *Arterioscler. Thromb. Vasc. Biol.* **17**, 483–489
55. Nguyen, M., Arkell, J., and Jackson, C.J. (1999) Thrombin rapidly and efficiently activates gelatinase A in human microvascular endothelial cells via a mechanism independent of active MT1 matrix metalloproteinase. *Lab. Invest.* **79**, 467–475
56. Pekovich, S.R., Bock, P.E., and Hoover, R.L. (2001) Thrombin-thrombomodulin activation of protein C facilitates the activation of progelatinase A. *FEBS Lett.* **694**, 129–132
57. Lafleur, M.A., Hollenberg, M.D., Atkinson. S.J., Knauper, V., Murphy, G., and Edwards, D.R. (2001) Activation of pro-(matrix metalloproteinase-2) (pro-MMP-2) by thrombin is membrane-type-MMP-dependent in human umbilical vein endothelial cells and generates a distinct 63 kDa active species. *Biochem. J.* **357**, 107–115
58. Maragoudakis, M.E., Kraniti, N., Giannopoulou, E., Alexopoulos, K., and Matsuokas, J. (2001) Modulation of angiogenesis and progelatinase A by thrombin receptor mimetics and antagonists. *Endothelium* **8**, 195–205
59. Liu, Y., Gilcrease, M.Z., Henderson, Y., Yuan, X.H., Clayman, G.L., and Chen, Z. (2001) Expression of protease-activated receptor 1 in oral squamous cell carcinoma. *Cancer Lett.* **169**, 173–180
60. Stetler-Stevenson, W.G., Aznavoorian, S., and Liotta, L.A. (1993) Tumor cell interactions with the extracellular matrix during invasion and metastasis. *Annu. Rev. Cell. Biol.* **9**, 541–573
61. Himelstein, B.P., Canete-Soler, R., Bernhard, E.J., Dilks, D.W., and Muschel, R.J. (1994) Metalloproteinases in tumor progression: the contribution of MMP-9. *Invasion Metastasis.* **14**, 246–258
62. Bernhard, E.J., Gruber, S.B., and Muschel, R.J. (1994) Direct evidence linking expression of matrix metalloproteinase 9 (92-kDa gelatinase/collagenase) to the metastatic phenotype in transformed rat embryo cells. *Proc. Natl Acad. Sci. USA* **91**, 4293–4297
63. MacDougall, J.R., and Matrisian. L.M. (1995) Contribution of tumor and stromal matrix metalloroteinases to tumor progression, invasion and metastasis. *Cancer Metastasis Rev.* **14**, 351–362
64. Hua, J. and Muschel, R.J. (1996) Inhibition of matrix metalloproteinase 9 expression by a ribozyme blocks metastasis in a rat sarcoma model system. *Cancer Res.* **56**, 5279–5284
65. Kim, J., Yu, W., Kovalski, K., and Ossowski, L. (1998) Requirement for specific proteases in cancer cell intravasation as revealed by a novel semiquantitative PCR-based assay. *Cell* **94**, 353–362
66. Hahn-Dantona, E., Ramos-DeSimone, N., Sipley, J., Nagase, H., French, D.L., and Quigley, J.P. (1999) Activation of proMMP-9 by a plasmin/MMP-3 cascade in a tumor cell model. Regulation by tissue inhibitors of metalloproteinases. *Ann. N. Y. Acad. Sci.* **878**, 372–387
67. John, A. and Tuszynski, G. (2001) The role of matrix metalloproteinases in tumor angiogenesis and tumor metastasis. *Pathol. Oncol. Res.* **7**, 14–23
68. Giannelli, G. and Antonaci, S. (2002) Gelatinases and their inhibitors in tumor metastasis: from biological research to medical applications. *Histol. Histopathol.* **17**, 339–345
69. Fernandez-Patron, C., Zhang, Y., Radomski, M.W., Hollenberg, M.D., and Davidge, S.T. (1999) Rapid release of matrix metalloproteinase (MMP)-2 by thrombin in the rat aorta: modulation by protein tyrosine kinase/phosphatase. *Thromb. Haemost.* **82**, 1353–1357
70. Duhamel-Clérin, E., Orvain, C., Lanza, F., Cazenave, J.P., and Klein-Soyer, C. (1997) Thrombin receptor-mediated increase of two matrix metalloproteinases, MMP-1 and MMP-3, in human endothelial cells. *Arterioscler. Thromb. Vasc. Biol.* **17**, 1931–1938
71. Liu, W.H., Chen, X.M., and Fu, B. (2000) Thrombin stimulates MMP-9 mRNA expression through AP-1 pathway in human mesangial cells. *Acta. Pharmacol. Sin.* **21**, 641–645
72. Yoshida, E., Verrusio, E.N., Mihara, H., Oh, D., and Kwaan, H.C. (1994) Enhancement of the expression of urokinase-type plasminogen activator from PC-3 human prostate cancer cells by thrombin. *Cancer Res.* **54**, 3300–3304
73. Benezra, M., Vlodavsky, I., and Bar-Shavit, R. (1992) Thrombin enhances degradation of heparan sulfate in the extracellular matrix by tumor cell heparanase. *Exp. Cell Res.* **201**, 208–215

Expression of Annexin A3 in Primary Cultured Parenchymal Rat Hepatocytes and Inhibition of DNA Synthesis by Suppression of Annexin A3 Expression Using RNA Interference

Shingo NIIMI,*[,a] Mizuho HARASHIMA,[b] Masaru GAMOU,[b] Masashi HYUGA,[a] Taiichiro SEKI,[b] Toyohiko ARIGA,[b] Toru KAWANISHI,[a] and Takao HAYAKAWA[c]

[a] *Division of Biological Chemistry and Biologicals, National Institute of Health Sciences; 1–18–1 Kamiyoga, Setagaya-ku, Tokyo 158–8501, Japan:* [b] *Department of Nutrition and Physiology, Nihon University College of Bioresource Sciences; Kameino, Fujisawa 252–8510, Japan: and* [c] *Deputy Director General, National Institute of Health Sciences; 1–18–1 Kamiyoga, Setagaya-ku, Tokyo 158–8501, Japan.*

Received October 30, 2004; accepted January 5, 2005; published online January 7, 2005

Annexin A3 is a member of the lipocortin/annexin family, which binds to phospholipids and membranes in a Ca^{2+}-dependent manner. Although annexin A3 has various functions *in vitro*, its cellular significance is completely unknown. Annexin A3 is not found in rat liver *in vivo*. In the present study, we investigated the expression of annexin A3 in primary cultured parenchymal rat hepatocytes. Annexin A3 protein was detected in 48-h, but not 2.5-h, cultured hepatocytes using Western blot analysis. The annexin A3 level further increased after an additional 24 h of culture. Annexin A3 mRNA was not detected in 2.5-h cultured hepatocytes but was detected 22 h after the start of culture by RT-PCR analysis, reaching a maximum value after 48 h of culture. To define the role of Annexin A3 in DNA synthesis, RNA interference was used to reduce annexin III gene expression in hepatocytes. The transfection of small interfering RNAs targeting annexin A3 in the hepatocytes reduced the corresponding mRNA and protein expression by approximately 80% and more than 90%, respectively, at 24 h after transfection. In the annexin A3 small interfering RNAs-transfected cells, DNA synthesis, as assessed by [^{3}H]thymidine incorporation, decreased by approximately 70% not only in the control cultures, but also in the hepatocyte growth factor- or epidermal growth factor-treated cells. These findings show that annexin A3 is expressed in primary cultured parenchymal rat hepatocytes and that the suppression of annexin A3 expression using RNA interference inhibits DNA synthesis.

Key words annexin A3; RNAi; DNA synthesis; primary cultured hepatocyte; hepatocyte growth factor (HGF); epidermal growth factor (EGF)

Annexin (Anx) A3 is also called "lipocortin 3" or "placental anticoagulant protein 3" (PAP-III)[1] and is a member of the lipocortin/annexin family, which binds to phospholipids and membranes in a Ca^{2+}-dependent manner.[2—4] AnxA3 has been shown to have anticoagulant and anti-phospholipase A_2 properties *in vitro*[5] and to promote the Ca^{2+}-dependent aggregation of isolated specific granules from human neutrophils.[6] Although the physiological functions of other annexins have been recently clarified in knock-out and transgenic models,[7—14] the functions of AnxA3 are completely unknown.[15]

Recently, we found that AnxA3 protein and its mRNA are not expressed in isolated parenchymal rat hepatocytes.[16,17] Consistent with these findings, AnxA3 protein and its mRNA are not detectable by Western blot analysis and Northern blot analysis in rat liver.[18—21] However, there have been no reports on the behavior of AnxA3 in primary cultured parenchymal rat hepatocytes. In the present study, we investigated the expression and function of AnxA3 in cultured parenchymal rat hepatocytes.

MATERIALS AND METHODS

Materials Recombinant human hepatocyte growth factor (HGF) was purchased from R&D systems (Minneapolis, MN, U.S.A.). Mouse epidermal growth factor (EGF) was purchased from Wako (Osaka, Japan). [^{3}H]thymidine (79.9 Ci/mmol) was purchased from PerkinElmer (Boston, MA, U.S.A.). Rabbit anti-human ANXA3 antibody serum was a generous gift from Dr. F. Russo-Marie and Dr. C. Raguenness-Nicol.

Cell Isolation and Monolayer Cultures Parenchymal hepatocytes were isolated from adult male Wistar rats, weighing 180—200 g, by *in situ* perfusion of the liver with collagenase.[22] All animal care and procedure protocols were approved by the institutional care committee. The cells were then suspended at a density of 2.5×10^5 cells/ml in Williams E medium (WE) containing 5% fetal bovine serum and 1 nM insulin and cultured at a density of 0.5×10^5 cells/cm^2 in a 6 cm dish and a 48-well microplate precoated with collagen type-I AC in a humidified chamber at 37 °C in 5% CO_2 and 30% O_2 in air. Cells plated in the 6-cm dish and 48-well microplate were used to prepare total cellular extracts or total RNA and to measure DNA synthesis, respectively. After 2.5 h of culture, the medium was replaced with a serum- and hormone-free medium containing aprotinin (1 μg/ml).

Western Blot Analysis Cell lysates were prepared using a modification of a previously described method.[23] The cells were washed with phosphate-buffered saline (PBS) followed by buffer A (50 mM Tris–HCl [pH 7.5], 150 mM NaCl, and 10 mM EDTA). The cells were then harvested after the addition of 20 μl of buffer A. The cells were suspended, shaken for 15 min at room temperature, and sonicated five times for 15 s each time while in an ice bath after the addition of 1/5 [v/v] of 5×buffer A containing 2.5% Triton X-100 and 1/100 [v/v] of a protease inhibitor cocktail (SIGMA). After centrifugation at $100000\times g$, the cytosolic fraction (about 25 μg) was subjected to sodium dodecyl sulfate-polyacrylamide gel

* To whom correspondence should be addressed. e-mail: niimi@nihs.go.jp

electrophoresis on a 10% gel and electroblotted to a PVDF membrane (GVHP; Millipore). After blocking the membrane with 5% skimmed milk, a Western blot analysis was performed using rabbit anti-human AnxA3 antibody serum at a dilution of 1 : 18000; detection was performed using the ECL detection system (Amersham Bioscience).

Reverse Transcription Polymerase Chain Reaction Analysis Total RNA was exctracted from the cells using Trizol reagent (Invitrogen) according to the manufacturer's protocols. Approximately 3 μg of RNA per sample was reverse-transcribed using the THERMOSCRIPT™ RT-PCR System (Invitrogen) and oligo$(dT)_{20}$ in a final volume of 40 μl, according to the manufacturer's protocols. Subsequently, 1 μl of cDNA was polymerase chain reaction (PCR)-amplified using the THERMOSCRIPT™ RT-PCR System (Invitrogen) in a final volume of 20 μl per reaction, according to the manufacturer's protocols, for 14—23 cycles of denaturation for 30 s at 94 °C, annealing for 30 s at 60 °C, and polymerization for 1 min at 72 °C using Anx AIII or glyceraldehyde 3-phosphate dehydrogenase (GAPDH) cDNA specific primers under linear conditions. The PCR products were separated on a 2% agarose gel, stained with SYBR Green I, and visualized and analyzed with a FluorolImager 595 (Amersham Bioscience). A computer assisted-analyzer was used to quantitatively analyze the signals, and the signals were normalized to the signal of a house keeping gene, the gene coding GAPDH. The sequences of the AnxA3 primers were as follows: 5′-CAAATTCACCGAGATCCTGT-3′ and 5′-TGCTGGAGTGCTGTACGAAA-3′. The sequences of the GAPDH primers were as follows: 5′-ACCACAGTCCATGCCATCAC-3′ and 5′-TCCACCACCTGTTGCTGTA-3′.[24] The PCR product specificity was confirmed by DNA sequence analysis using an ABI Prism 377 DNA Sequencer (Applied Biosystems, Foster City, CA, U.S.A.).

Preparation and Transfection of Small Interfering RNAs Targeting AnxA3 Small interfering RNAs (siRNAs) targeting rat AnxA3 were designed according to the guidelines of the "Dharmacon siDESIGN Center" (www.dharmacon.com) and obtained from Dharmacon Research (Lafayette) in annealed and lyophilized forms. The target sequences were localized at positions, 493 and 690 bps downstream of the start codon. The sequences of each siRNA pair were as follows: AnxA3 siRNA 1, 5′-GAG ACG AAA GCC UGA AAG UdTdT-3′ and ACU UUC AGG CUU UCG UCU cdTdT-3′; ANXA3 siRNA 2, 5′-GGA GAA UUA UCU GGG CAU UdTdT-3′ and AAU GCC CAG AUA AUUCUC cdTdT-3; and control siRNA, 5′-ACU CUA UCU GCA CGC UGA CUU-3′ and 5′-P G UCA GCG UGC AGA UAG AGU UU-3′. No homology between any relevant mammalian gene and the control siRNA was observed. These siRNAs were dissolved in an RNase-free solution provided by Dharmacon Research at a concentration of 20 μM. After 20 h of cell culture, the medium was replaced with WE containing aprotinin (1 μg/ml) immediately prior to transfection. Transfection with siRNA was performed using SiFector (B-bridge), according to the user guidelines. Sixty microliters of both AnxA3 siRNA 1 and 2 were diluted with OPTI-MEM (Invitrogen) to a final volume of 400 μl. Sixty-four microliters of SiFector was also diluted in OPTI-MEM to a final volume of 400 μl, then suspended and incubated at room temperature for 5 min. Next, the diluted siRNA was combined with SiFector, and the mixture was incubated at room temperature to allow the siRNA-SiFector complex to form. Eight hundred microliters of the siRNA-SiFector complex was added to the cultures (6-cm dish). For the 48-well plates, the siRNA-SiFector complex was prepared as described above except that the volume of each solution per well was scaled down to 1/16.

Measurement of [^{3}H]thymidine Incorporation After 20 h of culture, the medium was replaced with hormone-free medium containing aprotinin (1 μg/ml) and 0.1% bovine serum albumin (BSA), and EGF (2 ng/ml) or HGF (20 ng/ml) was added. After 1 h, 50 μl of siRNA-SiFector complex, prepared as described above, was added to the wells. After another 24 h, [^{3}H]thymidine (0.626 μCi) and thymidine (676.6 ng) were added, and 10 μg/ml of aphidicolin was added to some wells at the same time. The cells were then cultured for another 24 h. [^{3}H]thymidine incorporation was measured as described previously.[25] The difference between the radioactivity in the hot-trichloroacetic acid soluble fraction with and without aphidicolin was calculated as dpm/mg protein. Cell protein was measured using a previously described method,[26] with BSA used as a standard.

RESULTS

Expression of AnxA3 during Culture At first, we investigated the expression of AnxA3 in primary cultured parenchymal rat hepatocytes. AnxA3 protein was not detected by Western blot analysis 2.5 and 24 h after the start of culture but was detected after 48 h of culture (Fig. 1A). The level after 72 h of culture was approximately 1.6-fold higher than that after 48 h of culture (Fig. 1B). AnxA3 mRNA was not detected by reverse transcription (RT)-PCR in cultured hepatocytes after 2.5 h of culture but was significantly detected after 22 h of culture (Fig. 2A), reaching a maximum value after 48 h of culture (Fig. 2B). These results indicate

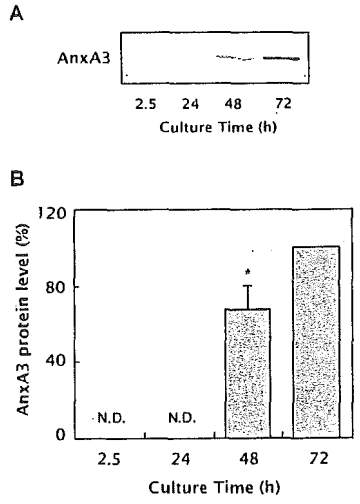

Fig. 1. Expression of AnxA3 Protein during Culture

(A) The data shown are representative of the Western blot analysis results. Cells lysates were prepared from the cells at the indicated times and used for the Western blot analysis. (B) The intensity of each band was quantified, and the results are shown relative to the value of cells cultured for 72 h. The data are expressed as the mean±S.D. of 3 experiments. *$p<0.01$, compared with the value of cells cultured for 72 h. N.D., not detected.

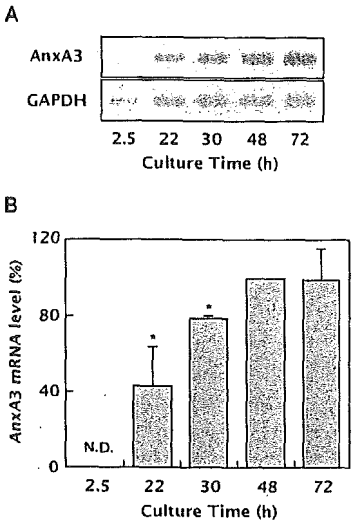

Fig. 2. Increase in AnxA3 mRNA Level during Culture

(A) The data shown are representative of the RT-PCR analysis results. Total RNA was prepared from the cells at the indicated times and used for the RT-PCR analysis. (B) The intensity of each band was quantified, and the results are shown relative to the value of cells cultured for 48 h. The data are expressed as the mean±S.D. of 3 experiments. *$p<0.01$, compared with the value of cells cultured for 48 h. N.D., not detected.

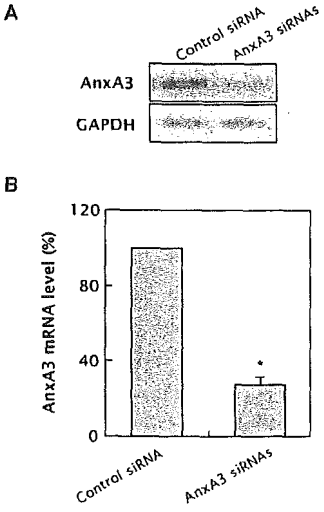

Fig. 3. Suppression of Increase in AnxA3 mRNA Level during Culture with RNAi

(A) The data shown are representative of the RT-PCR analysis results. Total RNA was prepared from the cells 1 d after siRNA transfection and used for the RT-PCR analysis. (B) The intensity of each band was quantified, and the results are shown relative to the value of cells transfected with control siRNA. The data are expressed as the mean±S.D. of 3 experiments. *$p<0.01$, compared with the value of cells transfected with control siRNA.

that the expression of AnxA3 is regulated by its mRNA level.

Suppression of AnxA3 Expression Using RNA Interference Next, we attempted to suppress AnxA3 expression by RNA interference (RNAi) to examine the role of ANXA3 in the cultured hepatocytes. AnxA3 mRNA expression was markedly reduced by treatment with AnxA3 siRNAs, compared with the expression after treatment with control siRNA, 1 d after the transfection (Fig. 3A), with an inhibition of approximately 80% (Fig. 3B). Furthermore, the AnxA3

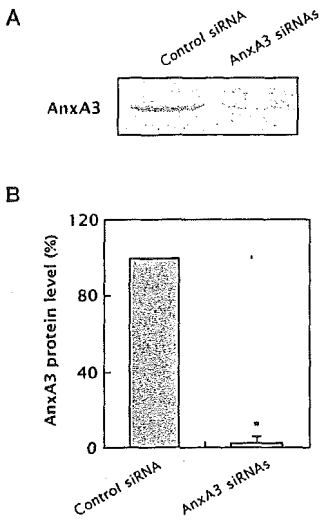

Fig. 4. Suppression of AnxA3 Protein Expression during Culture with RNAi

(A) The data shown are representative of the Western blot analysis results. Cells lysates were prepared from the cells 1 d after siRNA transfection and used for the Western blot analysis. (B) The intensity of each band was quantified, and the results are shown relative to the value of cells transfected with control siRNA. The data are expressed as the mean±S.D. of 3 experiments. *$p<0.01$, compared with the value of cells transfected with control siRNA.

protein level was also reduced by the treatment with AnxA3 siRNAs compared with the level after treatment with control siRNA (Fig. 4A), with an inhibition of more than 95% (Fig. 4B). On the other hand, the control siRNA had almost no effect on AnxA3 protein and mRNA levels compared with those treated with SiFector alone (data not shown). Neither the control nor AnxA3 siRNAs caused any cytotoxic effects, as observed microscopically or by the quantification of the total amount of protein in each sample (data not shown). These results indicate that AnxA3 siRNAs efficiently and specifically, inhibit the expression of AnxA3 in primary cultured parenchymal rat hepatocytes.

Inhibition of DNA Synthesis by Suppression of AnxA3 Expression Using RNAi Finally, we examined the role of AnxA3 in DNA synthesis by suppressing AnxA3 expression using RNAi. EGF (2 ng/ml) and HGF (20 ng/ml) stimulated DNA synthesis by approximately 7-fold and 9-fold, respectively in hepatocytes treated with control siRNA (Fig. 5). The stimulations were inhibited to approximately 70% by treatment with AnxA3 siRNAs. Similar results were also obtained in the control cells, whereas the control siRNA had almost no effect on DNA synthesis, compared with the effect in cells treated with SiFector alone (data not shown).

DISCUSSION

In the present study, we showed for the first time that AnxA3 is expressed in cultured parenchymal rat hepatocytes and that the inhibition of AnxA3 expression by RNAi resulted in a significant inhibition of DNA synthesis, suggesting that the expression of AnxA3 is necessary for DNA synthesis in primary cultured parenchymal rat hepatocytes.

Hepatocytes placed under culture conditions, are known to acquire a growth potential characterized by the enhancement of DNA synthesis, which is caused by several growth

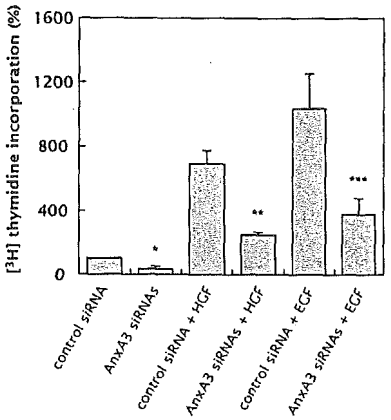

Fig. 5. Inhibition of DNA Synthesis by RNAi

The results are shown relative to the value of control cultured cells transfected with control siRNA. The data are expressed as the mean±S.D. of duplicate wells in 3 experiments. *$p<0.01$, compared with the value of control cultured cells transfected with control siRNA. **$p<0.01$, compared with the value of cells cultured in the presence of HGF and transfected with control siRNA. ***$p<0.01$, compared with the value of cells cultured in the presence of EGF and transfected with control siRNA. The mean±S.D. of [^{3}H]thymidine incorporation in the control cultured cells transfected with control siRNA was $9.72\times10^4\pm0.68\times10^4$ dpm/mg protein.

factors.[27,28] Our present findings suggest that the expression of AnxA3 is partly necessary for hepatocytes to acquire a growth potential under culture conditions. In fact, the enhanced expression of AnxA3 has been observed in hepatocellular carcinoma cell lines.[29] In addition, we discovered that the enhanced expression of Anx3 was observed in the proliferative hepatocytes after carbon tetrachloride-induced rat liver damage (unpublished observations).

As for other annexins, several findings concerning the relation of AnxA1 to hepatocyte growth has been reported as described below. The suppression of AnxA1 expression using antisense technology inhibited proliferation in a mouse hepatocyte cell line.[30] AnxA1 increased in the proliferative hepatocytes after carbon tetrachloride-induced rat liver damage or a partial hepatectomy and in hepatocellullar carcinoma tissue.[31,32]

Although the mechanism of action of AnxA3 on DNA synthesis is presently uncertain, the target of AnxA3 may be a common signal transduction pathway, and not necessarily a constitutive or growth factor-mediated one, because the suppression of AnxA3 expression using RNAi not only inhibited the control of DNA synthesis, but also EGF- or HGF-stimulated DNA synthesis, almost to a similar level. In this respect, the findings described below may be relevant to speculations on the mechanism of action of AnxA3 on DNA synthesis. The growth factor-mediated enhancement of hepatocyte growth consists of several signal transduction pathways.[33] The activation of cytosolic phospholipase A_2 ($cPLA_2$) by MAP kinase liberates arachidonic acid from phospholipids and is followed by the generation of prostaglandins, mediators of DNA synthesis, *via* cyclooxygenase. Interestingly, the suppression of AnxA1 expression using antisense technology inhibited $cPLA_2$ activity in a mouse hepatocyte cell line.[30] This report suggests that $cPLA_2$ must be phosphorylated by AnxA1 to become active. Additional evidence suggests that AnxA1 (275—346 aa), the region responsible for phospholipid binding is necessary for the interaction between AnxA1 and $cPLA_2$.[34] Further study is required to clarify the mechanism of action of AnxA3, including the possibility that AnxA3 positively modulates $cPLA_2$ activity, as in the case of AnxA1.

Acknowledgements This work was supported by grants for Health and Welfare Research from the Japanese Ministry of Health, Labor and Welfare.

REFERENCES

1) Crumpton M. J., Dedman J. R., *Nature* (London), **345**, 212 (1990).
2) Raynal P., Pollard H. B., *Biochim. Biophys. Acta*, **1197**, 63—93 (1994).
3) Gerke V., Moss S. E., *Physiol. Rev.*, **82**, 331—371 (2002).
4) Moss S. E., Morgan R. O., *Genome Biol.*, **5**, 219. 1—8 (2004).
5) Tait J. F., Sakata M., McMullen B. A., Miao C. H., Funakoshi T., Hendrickson L. E., Fujikawa K., *Biochemistry*, **27**, 6268—6276 (1988).
6) Ernst J. D., Hoye E., Blackwood R. A., Jaye D., *J. Clin. Invest.*, **85**, 1065—1071 (1990).
7) Gunteski-Hamblin A. M., Song G., Walsh R. A., Frenzke M., Boivin G. P., Dorn G. W., 2nd, Kaetzel M. A., Horseman N. D., Dedman J. R., *Am. J. Physiol.*, **270**, H1091—1100 (1996).
8) Kubista H., Hawkins T. E., Patel D. R., Haigler H. T., Moss S. E., *Curr. Biol.*, **9**, 1403—1406 (1999).
9) Srivastava M., Atwater I., Glasman M., Leighton X., Goping G., Caohuy H., Miller G., Pichel J., Westphal H., Mears D., Rojas E., Pollard H. B., *Proc. Natl. Acad. Sci. U.S.A.*, **96**, 13783—13788 (1999).
10) Herr C., Smyth N., Ullrich S., Yun F., Sasse P., Hescheler J., Fleischmann B., Lasek K., Brixius K., Schwinger R. H., Fassler R., Schroder R., Noegel A. A., *Mol. Cell. Biol.*, **21**, 4119—4128 (2001).
11) Song G., Harding S. E., Duchen M. R., Tunwell R., O'Gara P., Hawkins T. E., Moss S. E., *Faseb. J.*, **16**, 622—624 (2002).
12) Roviezzo F., Getting S. J., Paul-Clark M. J., Yona S., Gavins F. N., Perretti M., Hannon R., Croxtall J. D., Buckingham J. C., Flower R. J., *J. Physiol. Pharmacol.*, **53**, 541—553 (2002).
13) Hannon R., Croxtall J. D., Getting S. J., Roviezzo F., Yona S., Paul-Clark M. J., Gavins F. N., Perretti M., Morris J. F., Buckingham J. C., Flower R. J., *Faseb. J.*, **17**, 253—255 (2003).
14) Croxtall J. D., Gilroy D. W., Solito E., Choudhury Q., Ward B. J., Buckingham J. C., Flower R. J., *Biochem. J.*, **371**, 927—935 (2003).
15) Rand J. H., *N. Engl. J. Med.*, **340**, 1035—1036 (1999).
16) Niimi S., Hyuga M., Harashima M., Seki T., Ariga T., Kawanishi T., Hayakawa T., *Biol. Pharm. Bull.*, **27**, 1864—1868 (2004).
17) Niimi S., Oshizawa T., Yamaguchi T., Harashima M., Seki T., Ariga T., Kawanishi T., Hayakawa T., *Biochem. Biophys. Res. Commun.*, **300**, 770—774 (2003).
18) Kaetzel M. A., Hazarika P., Dedman J. R., *J. Biol. Chem.*, **264**, 14463—14470 (1989).
19) Comera C., Rothhut B., Cavadore J. C., Vilgrain I., Cochet C., Chambaz E., Russo-Marie F., *J. Cell. Biochem.*, **40**, 361—370 (1989).
20) Kristensen B. I., Kristensen P., Johnsen A. H., *Int. J. Biochem.*, **25**, 1195—1202 (1993).
21) Pepinsky R. B., Tizard R., Mattaliano R. J., Sinclair L. K., Miller G. T., Browning J. L., Chow E. P., Burne C., Huang K. S., Pratt D., Wachter L., Hession C., Frey A. Z., Wallner B. P., *J. Biol. Chem.*, **263**, 10799—10811 (1988).
22) Tanaka K., Sato M., Tomita Y., Ichihara A., *J. Biochem.* (Tokyo), **84**, 937—946 (1978).
23) Romisch J., Schuler E., Bastian B., Burger T., Dunkel F. G., Schwinn A., Hartmann A. A., Paques E. P., *Blood Coagul. Fibrinolysis*, **3**, 11—17 (1992).
24) Uno S., Nakamura M., Seki T., Ariga T., *Biochem. Biophys. Res. Commun.*, **239**, 123—128 (1997).
25) Niimi S., Horikawa M., Seki T., Ariga T., Kobayashi T., Hayakawa T., *Biol. Pharm. Bull.*, **25**, 437—440 (2002).
26) Bradford M. M., *Anal. Biochem.*, **72**, 248—254 (1976).
27) Fausto N., Laird A. D., Webber E. M., *Faseb. J.*, **9**, 1527—1536 (1995).
28) Michalopoulos G. K., DeFrances M. C., *Science*, **276**, 60—66 (1997).
29) Liang R. C., Neo J. C., Lo S. L., Tan G. S., Seow T. K., Chung M. C., *J. Chromatogr. B Analyt. Technol. Biomed. Life Sci.*, **771**, 303—328 (2002).
30) de Coupade C., Gillet R., Bennoun M., Briand P., Russo-Marie F.,